NRC Publications Archive
Archives des publications du CNRC

Fire Performance of Houses. Phase I. Study of Unprotected Floor Assemblies in Basement Fire Scenarios. Part 3 - Results of Test UF-04 (Steel C-Joists)

Bénichou, N.; Su, J. Z.; Bwalya, A. C.; Lougheed, G. D.; Taber, B. C.; Leroux, P.; Kashef, A.; Thomas, J. R.

NRC Publications Archive Record / Notice des Archives des publications du CNRC :
https://nrc-publications.canada.ca/eng/view/object/?id=4e8c3654-4bfc-4abd-82b4-6b57fd20436c
https://publications-cnrc.canada.ca/fra/voir/objet/?id=4e8c3654-4bfc-4abd-82b4-6b57fd20436c

Questions? Contact the NRC Publications Archive team at
PublicationsArchive-ArchivesPublications@nrc-cnrc.gc.ca. If you wish to email the authors directly, please see the first page of the publication for their contact information.

Vous avez des questions? Nous pouvons vous aider. Pour communiquer directement avec un auteur, consultez la première page de la revue dans laquelle son article a été publié afin de trouver ses coordonnées. Si vous n'arrivez pas à les repérer, communiquez avec nous à PublicationsArchive-ArchivesPublications@nrc-cnrc.gc.ca.

National Research Council Canada

Conseil national de recherches Canada

National Research Council Canada   Conseil national de recherches Canada

NRC · CNRC

Fire Performance of Houses

Phase I

Study of Unprotected Floor Assemblies in Basement Fire Scenarios

Part 3 – Results of Test UF-04 (Light-Gauge Steel C-Joists)

Research Report: IRC-RR-248

Date: March 31, 2009

Authors: N. Bénichou, J.Z. Su, A.C. Bwalya, G.D. Lougheed, B.C. Taber, P. Leroux, A.H. Kashef, J.R. Thomas

INSTITUTE FOR RESEARCH IN CONSTRUCTION
Fire Research Program

TABLE OF CONTENTS

NRC·CNRC

NRC·CNRC

LIST OF FIGURES

NRC·CNRC

LIST OF TABLES

ABSTRACT

This report documents part of the research project involving a series of full-scale fire experiments in a test facility that simulated a two-storey single-family house with a severe, fast growing fire originating in an unfinished basement to study the fire performance of the floor/ceiling assembly constructed over the basement. The report presents the results and analysis of Test UF-04 carried out in the test house with an unprotected steel C-joist floor/ceiling assembly above the basement with an open basement doorway (no door in the doorway leading from the first storey to the basement). A number of measurements were taken at various locations during the test such as temperatures, smoke alarm activation times, smoke optical density, floor deflection and concentrations of CO, CO_2 and O_2. For this test, untenable conditions on the upper storeys were reached before structural failure of the test floor assembly.

NRC·CNRC

FIRE PERFORMANCE OF HOUSES

PHASE I

STUDY OF UNPROTECTED FLOOR ASSEMBLIES IN BASEMENT FIRE SCENARIOS

Part 3 – Results of Test UF-04 (Light-Gauge Steel C-Joists)

N. Bénichou, J.Z. Su, A.C. Bwalya, G.D. Lougheed, B.C. Taber, P. Leroux, A.H. Kashef and J.R. Thomas

1   INTRODUCTION

1.1   Background

Risk of fires in buildings and concerns about their potential consequences are always present. Canada's fire death rate has continuously declined for the last three decades; much of this decline is attributed to the introduction of residential smoke alarms (this is also the case in the United States). With the advent of new materials and innovative products for use in construction of single-family houses, there is a need to understand what impacts these materials and products will have on occupant life safety under fire conditions and a need to develop a technical basis for the evaluation of their fire performance.

The National Building Code of Canada (NBCC) [1] generally intends that major structural load-bearing elements (floors, walls and roofs) have sufficient fire resistance to limit the probability of premature failure or collapse during the time required for occupants to evacuate safely [2]. Historically, the NBCC has not specified a minimum level of fire performance (fire resistance) of these structural elements in single-family houses.

In Canada, the Canadian Construction Materials Centre (CCMC) is called upon to evaluate the use of new materials and innovative construction products for compliance with the NBCC. Some of the more recent innovative structural products, seeking recognition for use in housing, are made of new composite and non-traditional materials that may have unknown fire behaviour. When evaluating new structural products, part of the CCMC challenge is related to the fact that no guidance or criteria are provided in the NBCC regarding the fire performance of structural systems used in single-family houses.

The Canadian Commission on Construction Materials Evaluation (CCCME) guides the operation of CCMC. Through the CCCME, CCMC sought the views of the Canadian Commission on Building and Fire Codes (CCBFC), which guides the development of the NBCC. After review and discussion, both the CCBFC and CCCME agreed that a study on the factors that affect the life safety of occupants of single-family houses should be conducted.

1.2 Goals of the Research

The National Research Council of Canada Institute for Research in Construction (NRC-IRC) undertook research into fires in single-family houses to understand the impact of residential construction products and systems on occupant life safety.

This research project sought to achieve the following goals:
1. To determine the significance of the fire performance of structural materials used in houses to the life safety of occupants.
2. To identify methods of measuring the fire performance of unprotected structural elements used in houses.
3. To measure and establish the fire performance of traditional house construction to facilitate the evaluation of the fire performance of innovative construction products and systems.

1.3 General Research Approach

Figure 1 shows a possible chronological sequence of relevant critical events that might occur in a fire scenario. It is acknowledged that the chronology of the occurrence of events may differ, and in some cases can shift in ordering.

Figure 1. Possible chronological sequence of events affecting the life safety of occupants in a fire situation

The research sought to establish, through experimental studies and using specific fire test scenarios, the typical sequence of the following events (measured from initiation of a fire), using a test facility intended to represent a typical code-compliant single-family house:
1. Sounding of smoke alarms (Event 1 as shown in Figure 1).
2. Loss of tenability within the environment of the first, second or subsequent storey(s) (Event 3).
3. Loss of integrity of the floor assembly and/or loss of its function as a viable egress route on the first or second storey(s)[1] (Event 4).

---

[1] The state of the egress route(s) on the first storey is relevant to the evaluation of the performance of the basement foundation walls and floor structure constructed over the basement;

NRC·CNRC

The research also sought to establish a basis for prediction or estimation of the required safe egress times expected for ambulatory occupants assuming a tenable indoor environment and a structurally sound evacuation route. A review of the literature on the waking effectiveness of occupants to smoke alarms, the delay time to start evacuation and the timing of escape in single-family houses was conducted. The objective of the review was to identify a range of estimated times families would take to awake, prepare and move out of their home after perceiving the sound of a smoke alarm during the night in winter conditions (Event 2 shown in Figure 1). This literature review was a separate but parallel study to the experimental studies. The results of the literature review are provided in Reference [3].

1.4   Scope of the Research Projects

The overall research consisted of a number of phases of experimental studies with each phase investigating a specified structural element based on specified fire scenarios.

Phase 1 (2004 to 2007) of the experimental study focused on basement fires and their impacts on the structural integrity of unprotected floor assemblies above a basement and the tenability conditions in a full-scale test facility. It is acknowledged that, a basement is not the most frequent site of household fires but it is the fire location that is most likely to create the greatest challenge to the structural integrity of the 1st storey structure, which typically provides the main egress routes. The study of fires originating in basements also provides a good model for the migration of combustion products throughout the house and its egress paths. The data collected during this phase of the project provided important indicators for identifying and evaluating the sequence for the occurrence of critical events shown in Figure 1.

This research focused on the life safety of occupants in single-family houses. The safety of emergency responders in a fire originating in single-family houses was not within the scope of this research project. Technical data collected during this research could aid in clarifying the potential risks associated with firefighting activities.

1.5   Content of this Document

This report documents the results of the initial phase of work involving an experimental study of the structural fire performance of the floor/ceiling assembly (1st floor) constructed over the basement level of a test house. Specifically, this report contains the data and analysis of Test UF-04 of the Phase I study carried out in the test house with an unprotected steel C-joist floor/ceilingassembly. This includes results on the fire scenarios, tenability, structural integrity, and the sequence of Events 1, 3 and 4, as illustrated in Figure 1.

---

the state of the egress route on the second storey is relevant to the evaluation of the performance of the above-grade wall structures and floor structure over the first storey.

2 EXPERIMENTAL STUDY

To undertake this research, NRC-IRC constructed a three-level experimental facility, representing a typical two-storey detached single-family house with a basement. The facility allows the study of structural fire performance, as well as smoke movement and tenability under fire conditions for single-family houses. The facility has a total floor area of approximately 95 m^2 per storey and is shown in Figure 2.

Figure 2. Three-storey facility

2.1 Geometry - Compartments in the Facility

2.1.1 Fire Compartment in Basement

The layout of the basement is shown in Figure 3. The basement was partitioned to create a fire room representing a 27.6 m2 basement living area, or about 1/4 of the total basement area. This compartment size was chosen based on a survey carried out by NRC [4]. The area of the basement that was not used for the fire compartment was blocked off during the fire tests. The height of the basement was 2.44 m. The ceiling clear height depended on the depth of the floor assembly being tested. A rectangular exterior opening measuring 2.0 m wide by 0.5 m high and located 1.8 m above the floor was provided in the south wall of the fire room. The size of the opening was chosen based on the results of the survey carried out by NRC [4]. A 0.91 m wide by 2.05 m high doorway opening located on the north wall of the fire room led into an empty stairwell enclosure (without a staircase). At the top of this stairwell, a 0.81 m wide by 2.05 m high doorway led into the first storey, as shown in Figure 4. This doorway either had no door (open basement doorway) or had a door in the closed position (closed basement doorway), depending on the scenario being studied. There is no requirement for a basement door in the NBCC. Section on "Openings and their States" provides more details.

4

NRC·CNRC

Figure 3. Basement level layout (dimensions in mm)

2.1.2   First Storey

The first storey had an open-plan layout with no partitions, as shown in Figure 4. A test floor assembly was constructed on the first storey directly above the fire room for each experiment.   The remainder of the floor on the first storey was constructed out of non-combustible materials. The height of the storey was about 2.44 m. As shown in Figure 4, this storey had 2 door openings: a door opening to the outside (dimensions of 0.89 m by 2.07 m) and a door opening that connected the basement to the first storey (dimensions of 0.81 m by 2.05 m). This storey also connected to the 2nd storey by a staircase in the middle of the storey area. This staircase to the second storey was not enclosed. The floor being tested was positioned in the southeast quarter of the first storey, on top of the fire compartment.

2.1.3   Second Storey

The layout of the second storey is shown in Figure 5. This storey was partitioned to contain two identical bedrooms with dimensions of 3.75 m by 4.47 m connected by a corridor with dimensions of 1.1 m x 4.45 m. The height of the storey was 2.44 m. In all tests, the door of the southeast bedroom remained closed whereas the door on the southwest bedroom was kept open. The size of the door openings was 0.81 m by 2.05 m. The remaining area of the second storey that was not used was blocked off during the fire tests.

NRC·CNRC

Figure 4. First storey layout (dimensions in mm)

Figure 5. Second storey layout (dimensions in mm)

6

NRC·CNRC

2.2   Lining Materials in Compartments

The compartments were lined with different materials. For the basement level, the walls of the fire compartment were lined with 12.7 mm thick regular gypsum board. There was no ceiling finish in the fire compartment, so the floor assembly, including both the framing supports (C-joists) and the underside of the subfloor (oriented strand board, OSB), was unprotected and exposed. For the first and second storeys, cement board covered the walls, and the ceilings were covered with 12.7-mm thick regular gypsum board. There was no finished floor in the 1st storey, so the upper surface of the OSB subfloor used on the floor assembly being tested was exposed. In the remainder of the compartment on the first storey, the floor was noncombustible. The OSB that was used for the subfloor was chosen on the basis of a study on the performance of different OSBs when exposed to fire [5].

2.3   Openings and their States

The openings included: on the basement level, a rough window opening; on the first storey, a door opening to the outside and a door opening at the top of the empty stairwell enclosure (contained no stairs) leading from the basement level; on the second storey, a door opening in the corridor at the top of the stairs leading from the first storey and door openings from the corridor leading to each of the two bedrooms. The size of all the doorways were typical of those used in housing. The single window opening in the basement (2.0 m x 0.5 m) represents an area equal to the size of two typical basement windows.

The doors on the door openings were inexpensive moulded-fibreboard hollow-core interior doors with minimum size styles and rails or solid-core exterior wood doors. The rough window opening in the basement level was covered with a noncombustible panel that could open at the appropriate time in each fire test.

At the start of a test, the rough window opening in the basement and the exterior door on the first storey leading to the outside were closed. Both were opened at critical times during a test (see Section 2.6 Testing Procedure). The doorway on the first storey leading to the basement had no door (open basement doorway) in Test UF-04. On the second storey, during the test, the door to the southwest bedroom was open, and the door to the southeast bedroom was closed.

There was no heating, ventilating and air-conditioning or plumbing system installed in the test house, i.e., no associated mechanical openings in the floor.

2.4   Fuel Load in the Fire Compartment

The selection of the fuel load and its arrangement in the fire compartment was a critical element in this experimental work. A study was conducted to select the fire scenario and fuel package, which was used in this phase of the project [6]. This fuel package consisted of a mock-up sofa constructed with 9 kg of exposed polyurethane foam (PUF),

the dominant combustible constituent of upholstered furniture, and 190 kg of wood cribs beside and underneath the mock-up sofa. A photograph of the fuel package is shown in Figure 6. The mock-up sofa was constructed with 6 blocks of flexible polyurethane foam (with a density of 32.8 kg/m^3) placed on a metal frame. Each block was 610 mm long by 610 mm wide and 100 mm or 150 mm thick. The 150-mm thick foam blocks were used for the backrest and the 100 mm thick foam blocks for the seat cushion. The PUF foam was used without any upholstery fabric that is used in typical upholstered furniture. The wood cribs were made with spruce lumber pieces, each piece measuring 38 mm x 89 mm x 800 mm. For the small cribs located under the mock-up sofa, four layers with six pieces per layer were used. The other two cribs used eight layers.

The placement of the fuel package in the basement fire compartment is illustrated in Figure 7. The mock-up sofa was located at the center of the floor area. The mock-up sofa was ignited in accordance with the ASTM 1537 test protocol [7] and the wood cribs provided the remaining fire load to sustain the fire for the desired period of time.

Figure 6. Fuel package

Figure 7. Arrangement of the fuel package in the fire compartment

(dimensions in mm)

2.5 Instrumentation in the Different Compartments and Exterior

The following is a summary of the instrumentation installed inside and around the exterior of the test facility.

2.5.1 Fire Compartment in Basement

The instrumentation in the basement fire room included the following:

- Four vertical arrays of thermocouples located at the quarter points of the fire room to measure temperatures at heights of 0.4, 0.9, 1.4, 1.9 and 2.4 m above the floor level.
- Thermocouples located at the basement exterior opening (window) to measure the temperature at the simulated window and the temperature of the gas plume after the mock-window was opened.
- A residential photoelectric smoke alarm located near the stairwell.
- Air velocity measurements at the basement exterior opening (window).
- Differential pressure measurement between the fire compartment and the exterior of the test facility, located 2.0 m above the floor.
- Video recording of the burning fuel package.
- Thermocouples measuring temperatures in the wood cribs.

The positioning of the instrumentation in the fire compartment on the basement level is shown in Figure 8.

NRC·CNRC

Figure 8. Fire Compartment instrumentation

2.5.2   First Storey

The instrumentation on the first storey included the following:

- Four vertical thermocouple arrays at the quarter points of the whole floor area.
- One vertical thermocouple array located at the door opening of the stairwell from the basement level.
- Gas sampling ports at the southwest quarter point, including:
  - $CO/CO_2/O_2$ at 0.9 m and 1.5 m above the floor.
  - Fourier Transform Infrared Spectroscopy (FTIR) at 1.5 m above the floor.
- Smoke density measurements at the southwest quarter point at 0.9 m and 1.5 m above the floor.
- Residential ionization and photoelectric smoke alarms located on the ceiling near the doorway to the basement.
- Air velocity measurements located at top of the basement stairwell at ceiling height and at 1.5 m above the floor.
- Differential pressure measurement between the fire compartment in the basement level and the first storey.
- Video recording from two locations.

The positioning of the instrumentation on the first storey is shown in Figure 9.

NRC·CNRC

Figure 9. First storey instrumentation

2.5.3 Second Storey

The instrumentation on the second storey included the following:

- One vertical thermocouple array in the corridor at the top of the stairs.
- One vertical thermocouple array in the center of each bedroom.
- Residential ionization and photoelectric smoke alarms located on the ceiling in the corridor at the top of the stairs.
- Residential ionization and photoelectric smoke alarms located on the ceiling at the centre of each bedroom.
- Gas analysis ($CO/CO_2/O_2$) in the corridor at the top of the stairs at 0.9 m and 1.5 m above the floor.
- Smoke density measurements in the corridor at the top of the stairs at 0.9 m and 1.5 m above the floor.
- Air velocity measurements located at the top of the stairs at ceiling height and at 1.5 m above the floor.
- Video recording in the corridor.

The positioning of the instrumentation on the second storey is shown in Figure 10.

NRC·CNRC

Figure 10. Second storey instrumentation

2.5.4   Exterior

Instrumentation of the facility exterior included the following:

- Air velocity measurements located at the basement window opening.
- Air velocity measurements located at the exterior door opening on the first storey.
- Video recording of the exterior window opening in the fire compartment on the basement level and the exterior door opening on the first storey.

2.6   Testing Procedure

The mock-up sofa was ignited in accordance with the ASTM 1537 test protocol [7] and data was collected at 5 s intervals throughout each test.

The non-combustible panel that covered the fire room's exterior rough window opening during the initial stage of each test was manually removed when the temperature measured at the top-center of the opening reached 300°C. The removal of the panel was to provide ventilation air necessary for combustion.

The exterior door on the first storey was opened at 180 s after ignition and left open, simulating a situation where some occupants, who would have been in the test house,

NRC·CNRC

escaped leaving the exterior door open while other occupants may still have been inside the house.

The test was terminated by extinguishing the fire using a manually operated sprinkler system when one of the following occurred (singly or in combination):
- Excessive flame penetration through the floor assembly;
- Structure failure of any part of the floor assembly;
- Compromise of safety of the test facility.

2.7   Construction Details of the Floor Assembly

Eleven full-scale floor assemblies were tested in this first phase of the project. In each test, the floor assembly was installed in the three-storey test facility to create the ceiling portion over the fire compartment in the basement level. The floor assemblies had no ceiling sheathing attached on the underside, leaving the framing members and the subfloor exposed and unprotected from exposure to the fire from the burning fuel package.

For each type of floor assembly tested, the floor joist/truss spans were either chosen from the appendices of the NBCC or calculated based on the ultimate and serviceability limit states. Therefore, the floor joists/trusses could either span the entire length of the fire compartment space or require an intermediate beam support for shorter spans. When designing the assembly, various aspects were considered including what is typically used for framing and subfloor materials in housing today, consideration of serviceability limit states, typical spacing, typical spans, typical depths, etc. As well, the assembly was loaded at 50% of the specified load in the NBCC (see Section 2.9).

Details on the tested assembly (steel C-joists) are provided below.

2.7.1   Floor Assembly with Light-gauge Steel C-Joists

The test, documented in this report, was conducted using a steel frame floor assembly constructed using steel C-joists and an OSB subfloor. The overall dimensions of the C-joist assembly were 5250 mm by 5150 mm. Specific dimensions of the various components of the assembly are provided in Figure 11 to Figure 16.

The light-gauge steel C-joists were 203 mm by 41 mm, 1.438 mm (gauge 17), and were spaced at 400 mm on centre (see Figure 11). Based on calculations of maximum strength and deflection, the C-joist span length chosen was 4.477 m (see Figure 11). Since the maximum span allowed for the steel C-joists does not extend across the entire length of the fire compartment, a beam was used as an intermediate support at the end of the 4.477-m span and a set of shorter C-joists were used to increase the span of the floor to extend to the end of the fire compartment. Figure 11, Figure 12 and Figure 13 show the details of the joist overlaps and the supporting beams. This assembly was constructed with blocking and continuous flat strap at the mid span and at the joist overlaps.

NRC·CNRC

Figure 11. Steel C-joist layout details (all dimensions in mm)

Steel C-joist 203 x 41 x 1.438 [800S162-54 (50)]
Steel C-joist overlap
#10-16 screws through stiffner and both C-joists
167
Stiffner inside the joist with the longer span length
Anchor bolts
C-joist secured to sill plate with 2-#8 wood screws

(North view)

Figure 12. Steel C-joist overlap details (all dimensions in mm)

#8-18 screws 19 long top and bottom of rim track
Rim track 203 x 32 x 1.438 [800T125-54 (50)]
Steel C-joist 203 x 41 x 1.438 [800S162-54 (50)]
Structural adhesive between C-joist and OSB
Web stiffener 32 x 92 x 1.146 x 194 long [362S125-43]
                                    centred over W200 beam
#10-16 screws 19 long
Anchor bolts
C-joist secured to sill plate with 2-#8 wood screws
Ceramic fibre blanket
Gypsum Board 12.7 thick
Cement Board 12.7 thick
Steel stud 89 deep
Glass fibre insulation 89 thick
Sheet metal 18 ga
Wall

(North view)

Figure 13. End connection details and supports (all dimensions in mm)

NRC·CNRC

The steel C-joist floor assembly was supported by three beams, which in turn, were supported by six columns (two columns for each beam). The beams were bolted to the columns, which were stiffened by bars and rested stably on the floor under the weight of the assembly and beams.

Figure 13 also shows the end connection details. Ceramic fibre blankets were used to fill any gaps between the assembly and the end walls. Ceramic fibre blankets were also used to protect the beams and columns so that they were not subjected to fire and would not fail during the test.

In the steel C-joist test assembly, rim tracks (headers) made of steel 203 mm by 32 mm and 1.438 mm thick, were placed at the east and west sides of the floors as shown in Figure 11. In the assembly, blocking-in, stiffeners and a continuous strap were used. Details of the C-joist layout are shown in Figure 11 and Figure 14.

Blocking-in detail B1

Blocking-in detail B2

Figure 14. Blocking-in details (all dimensions in mm)

NRC·CNRC

OSB was used as the subfloor material in the floor assembly. The specific OSB material used was selected based on a separate study documented in [5]. The subfloor panels were 15.1 mm thick in the assembly, with a full panel size being 1.2 x 2.4 m. The longer panel edges had a tongue and groove profile while the short panel edges were square-butt ends. Figure 15 shows the subfloor layout details. The screw pattern and description of screws used to attach the OSB panels to the steel C-joists and rim track are shown in Figure 16.

Figure 15. Subfloor layout details (all dimensions in mm)

Figure 16. Subfloor screw pattern and screw description (all dimensions in mm)

2.8   Instrumentation of the Floor Assembly

2.8.1   Temperatures in the Floor Assembly

Ninety-seven Type K (20 gauge) chromel-alumel thermocouples, with a thickness of 0.91 mm, were used for measuring temperatures at a number of locations throughout the assembly. The thermocouple locations on the unexposed and exposed sides of the assembly are shown in Figure 17 and Figure 18. These locations were chosen to monitor the conditions of the assembly at critical locations during the fire test.

Figure 17. Thermocouples locations (all dimensions in mm)

Figure 18. Thermocouples locations reflecting the different sections shown in Figure 17

2.8.2 Flame Penetration of the Floor Assembly

Flame penetration through the floor assembly is considered to be an initial indicator of the impending failure of the assembly. A device was developed and used for the test to better determine the time for flames to penetrate the floor. The special device consisted of a wire mesh placed at 3 locations on the unexposed surface of the floor assembly, specifically at three of the tongue and groove joints, as shown in Figure 19. A detailed description of the device is provided in [8].

NRC·CNRC

Figure 19. Wire mesh device to detect flame penetration (all dimensions in mm)

NRC·CNRC

2.8.3 Deflection of the Floor Assembly

The floor deflection was measured at 9 points. The measurement technique utilized 9 rods that were touching the tops of 9 concrete blocks placed on the unexposed surface of the floor assembly at the locations shown in Figure 20. This ensured that the downward movement of the subfloor was monitored during the fire exposure. The deflections were recorded using the electro-mechanical method described in reference [9].

Figure 20. Loading blocks and locations of the deflection measurement points on the unexposed side of the floor

2.9 Loading of the Floor Assembly

The load applied on the floor assemblies was equal to the self-weight (dead load) of the assembly plus an imposed load (live load) of 0.95 kPa (i.e., half of that prescribed by the NBCC [1] for residential occupancies, i.e., half of 1.90 kPa). The rationale to use this combination was based on the fact that in a fire situation, only part of the prescribed load is available. In fact, a number of international standards (Eurocode [10], New Zealand and Australian standards [11 and 12], and ASCE [13]) use a load combination similar to the one used in this study for fire design purposes. The total imposed load applied to the floor was equal to 0.95 kPa multiplied by the floor area; this is equivalent to approximately 25 kN

The loading method consisted of 144 concrete blocks (totalling 2490 kg) distributed uniformly on the floor as shown in Figure 20. The blocks were 190 x 190 x 390 mm (nominal 8" x 8" x 16") and weighed 17.3 kg each. To prevent the blocks from falling into

the basement and causing any damage, a restraining system was designed using a series of pipes attached to beams on both ends, which were secured to the steel frame of the 3-storey house, as shown in Figure 21. The pipes were inserted through the hollow cores of the concrete blocks prior to the fire test. The weight of the pipes was included in the total imposed load.

Figure 21. Device to hold the loading blocks

Calculations of the maximum imposed loads (live load) that the floors were capable of supporting (based on the span used and production of maximum allowable bending stress/deflection, whichever applies, calculated in accordance with CAN/ULC-S101 standard [14]) indicate that the floor had a large strength reserve. The calculated reserves in %, based on comparison of the loading requirement with maximum imposed loads, which govern in this case, are shown in Table 1.

Table 1. Reserve Live Load Capacity

Test Number	Imposed load (kPa)	Maximum imposed load (kPa)		Reserve of live load capacity (governed by strength) (%)	Reserve of live load capacity (governed by deflection) (%)
		Strength	Deflection		
UF-04	0.95	3.49	2.50	73	62

NRC·CNRC

3 RESULTS OF THE TEST

3.1 Recording of Results

Compartments and the floor assembly were instrumented with smoke alarms, thermocouples, gas analyzers (CO, CO_2 and O_2), smoke density instruments, pressure measurement instruments, and video cameras. The measurements of temperatures, gas concentrations, smoke density, and pressure were recorded at 5-second intervals using a Solotron data acquisition system.

In the following sections, discussions of the different recorded results are carried out. Figures showing various quantities have been organized as follows:

- Figure 22 to Figure 28 show the test results for temperatures vs. time in the compartments, and at different openings (basement window opening, door opening to the basement, door opening to the outside), and at the top of the stairs (between the basement and first storey, and between the first and second storeys).
- Figure 29 shows the test results for temperatures vs. time on the unexposed side of the floor assembly.
- Figure 30 shows the test results for temperatures vs. time on the exposed side of the floor assembly.
- Figure 32 shows the test results for deflection vs. time on the unexposed side of the floor assembly.
- Figure 33 shows the results from the flame-sensing devices.
- Figure 34 to Figure 38 show the smoke and gas measurement results (CO, CO_2, O_2 and optical density) and tenability conditions vs. time in the compartments.
- Figure 39 shows the test results for the sequence of fire events in Test UF-04.

Although velocity measurements were recorded at various openings during the experiments, they are not discussed in this report. However, these results may be useful for fire modeling purposes in the future.

3.2 Observations and Recordings

Table A 1 shows the test summary for UF-04. This includes a short description of the test, the times for various events, and the detection times for all smoke alarms that operated. The test was stopped after indications of either the structural or load-bearing failure of the floor.

3.3 Time-temperature Curves at Different Locations

3.3.1 Temperatures in the Compartments

In the following sections, the temperatures in the basement, first storey, and second storey are discussed. All thermocouple trees provided measurements at 0.4, 0.9, 1.4, 1.9 and 2.4 m above the floor level. Figure 22 to Figure 24 show these temperatures.

NRC·CNRC

3.3.1.1 Basement

Figure 22 (a, b, c, and d) shows the temperatures in the basement fire compartment at the 4 quarters, southeast (SE), southwest (SW), northeast (NE) and northwest (NW), respectively.

The temperatures rose to a maximum of 700 to 840ºC in the first 140 to 160 s, which was due to the burning of the mock-up sofa. As shown in the figures, the initial fire growth was faster at the 2.4 m height than the other heights because the hot smoke layer formed first at the ceiling and flames were also impinging on the ceiling initially.

Just after the maximum was reached, there was a slight decrease in temperatures because of the opening of the basement window at 120 s. The temperature decrease became larger after the opening of the exterior door on the first storey, which created a movement of air and smoke between the basement and first storey.

The fresh air coming from the basement window increased the combustion of the wood cribs, which caused the temperatures to increase steadily again, reaching a maximum of just under 900ºC.

Finally, the temperatures decreased again just after 460 s when the floor started falling and the test was ended. It should be noted that the temperature was lowest in the case of the NE thermocouple tree, which may be partially attributed to the fact that the NE corner was the least impacted by the fire, as it was farthest away from the fire source and that most of the hot gases were moving to the upper storeys through the SE to NW path.

The combustion was dominated by the mock-up sofa during the first 140 to 160 s, while the wood cribs and the subfloor provided the fuel for combustion after this period.

a) Basement SE quadrant

b) Basement SW quadrant

Figure 22 (a and b). TC Trees in the basement for UF-04

NRC·CNRC

c) Basement NE quadrant

d) Basement NW quadrant

Figure 22 (c and d). TC Trees in the basement for UF-04

NRC·CNRC

3.3.1.2 First storey

Figure 23 (a, b, c, and d) shows the temperatures measured at the thermocouple trees in the first storey at the 4 quarters, SE, SW, NE and NW, respectively. The temperatures steadily increased due to the heating of the floor from below and the hot gases and smoke migrating from the basement through the open basement doorway. The highest temperatures were recorded at the SE thermocouple tree because the fire in the basement was just underneath this tree. The temperatures measured at the other three thermocouple trees were similar. At around 400 to 440 s, there was a sharp increase in temperatures, which may be an indication of flame penetration through the floor. The peak temperatures were 760, 640, 440 and 400ºC at the SE, SW, NE and NW thermocouple trees, respectively. After 460 s, the temperatures started decaying because of the extinguishment of the fire.

3.3.1.3 Second storey

Figure 24 (a) and Figure 24 (b) show the temperatures in the SE and SW bedrooms, respectively for Test UF-04. The door to the SE bedroom was closed while the door to the SW bedroom was open. Ambient temperature was measured for about the first 220 s for the SE bedroom and 140 s for the SW bedroom. After this, the temperatures, at different heights within the rooms, start increasing. This increase was greater for the SW bedroom than the SE bedroom because the door to the SW bedroom was open. Maximum temperatures of about 40 and 180ºC were reached at 2.4 m height above the floor level in the SE and SW bedrooms, respectively. For the SW bedroom, the temperatures started decaying after the extinguishment of the fire was initiated.

a) 1st Storey SE quadrant

b) 1st Storey SW quadrant

Figure 23 (a and b). TC trees in the first storey for UF-04

NRC·CNRC

c) 1st Storey NE quadrant

d) 1st Storey NW quadrant

Figure 23 (c and d). TC trees in the first storey for UF-04

30

NRC·CNRC

a) 2nd Storey SE bedroom

b) 2nd Storey SW bedroom

Figure 24. TC trees in the second storey bedrooms for UF-04

31

3.3.2   Temperatures at the Window in the Basement

Five thermocouples were located in the basement window opening. Three were located along the vertical centreline of the opening, 125 mm from the bottom, 250 mm from the bottom and 375 mm from the bottom, respectively. The remaining two thermocouples were located 375 mm up from the bottom of the opening and 500 mm in from each side of the opening.

Figure 25 shows the temperatures recorded at the basement window. The temperatures increased sharply to 600ºC in the first 140 s. The window was opened after 120 s when the temperatures reached 300ºC. After 120 s, due to air entering and smoke exiting the basement window opening, the temperatures were scattered depending on whether or not the flames were touching the thermocouples (the bottom TC was probably below the neutral plane).

Figure 25. Temperatures at the window in the basement for UF-04

3.3.3   Temperatures on the First Storey at the Top of the Stairs from the Basement

Figure 26 shows the temperatures at the top of the stairs on the first storey at different heights. The conditions remained at ambient temperature for about the first 50 s. After this, temperatures, at different heights, started increasing due to the migration of hot gases and smoke from the basement to the upper storeys. A maximum temperature of about 900ºC was reached and then there was a decline in temperatures because the exterior door on the first storey was opened and fresh air entered the compartment. The temperatures then remained constant for a short time. After this, the temperatures at

NRC·CNRC

2.4 and 0.4 m levels started increasing again due to the extensive burning of the wood cribs and flame penetration through the floor. The temperatures started decaying around 460 s when extinguishment of the fire was initiated. The maximum temperature was not reached at the 2.4 m level but at the 0.9, 1.4 and 1.9 m levels. This is probably an indication that cooler air was entering into the basement at both the upper level and lower level of the basement doorway.

Figure 26. Temperatures on the first storey at the top of the stairs from the basement for UF-04

3.3.4   Temperatures on the Second Storey at the Top of the Stairs

Figure 27 shows the temperatures at the top of the stairs on the second storey at different heights for Test UF-04. The conditions remained at ambient temperature for about the first 130 s. After this, temperatures, at different heights, started increasing due to the migration of hot gases and smoke from the basement to the upper storeys. A maximum temperature of about 280ºC was reached at the 2.4 m height. The temperatures started decaying after the extinguishment of the fire was initiated.

NRC·CNRC

Figure 27. Temperatures on the second storey at the stairs for UF-04

3.3.5   Temperatures at the Outside Doorway on the First Storey

Figure 28 shows the temperatures outside the exterior door on the first storey. Ambient temperature was measured for about the first 100 s. After these times, the temperatures started increasing reaching 300ºC at 220 s due to smoke and hot fire gases exiting through the open exterior door. The temperature decreased at about 260 s. Just after 440 s, there was a sharp increase in temperatures (due probably to flame penetration through the floor producing more radiation and hot gases in the vicinity of the exterior door). The temperatures started decaying after about 460 s, after the extinguishment of the fire was initiated.

Figure 28. Temperatures at the outside doorway on the first storey for UF-04

3.3.6   Temperatures First Storey on the Unexposed Side of the Floor Assembly

Figure 29 (a and b) shows the temperatures measured by thermocouples (TCs) No. 1 to 9 and No. 92 through 97 located on the unexposed side (top) of the OSB subfloor in the floor assembly (see Figure 17 and Figure 18).   For TCs 1 to 9, the temperatures remained at ambient temperature for the first 180 s.   After this, the temperatures increased gradually until 350 s; thereafter, the temperatures show a faster rate of increase at all locations.   This faster increase in temperature rise was due to the positioning of the thermocouples in the vicinity of the fire.   This also is likely an indication that flames penetrated through the subfloor and the floor was being breached at many locations around 350 s.   The maximum temperature reached was about 720°C. Subsequently, the temperatures decreased after the extinguishment of the fire.

TCs No. 1 to 9 that were covered with insulated pads were closer to those areas of the floor assembly that were directly over the fire source; while the bare TCs No. 92 to 97 were around the perimeter of the floor assemblies. The temperatures measured with the bare TCs 92 to 97 were lower than those measured with the TCs covered by insulated pads.

It is worth mentioning that under standard fire test conditions (CAN/ULC-S101 and ASTM E 119 tests) [14], temperatures on the unexposed faces of specimens measured with uncovered TCs are always lower than those measured by TCs covered with insulated pads. In the standard tests [14], on the basis of temperature, floor failure is defined as a temperature rise of 140°C above ambient temperature for the average of the nine padded thermocouples or a temperature rise of 180°C above ambient temperature at any single point (padded thermocouple) on the unexposed side.

a) Unexposed TCs under insulated pad on top of subfloor.

b) Bare TCs on the unexposed (top) side of subfloor.

Figure 29. Temperatures at the unexposed side of subfloor for UF-04

NRC·CNRC

3.3.7 Temperatures on the Exposed Side of the Floor Assembly

The location of each grouping of thermocouples is identified by the Section label (A, B, C, D, and E) and the C-joist space shown on Figure 17 and Figure 18. For example, C-1 is the group of thermocouples located along Section C in C-joist Cavity 1.

For the thermocouple groupings within the C-joist cavities with seven thermocouples at each section, the individual thermocouples are identified as follows: bottom of north C-joist (Bot SJ North (1)), mid-height of north C-joist (Mid SJ North (2)), between the north C-joist and the subfloor (SF/SJ North (3), on the subfloor mid-distance between the two C-joists (SF/Cav (4)), between the south C-joist and the subfloor (SF/SJ South (5), mid-height of south C-joist (Mid SJ South (6)) and bottom of south C-joist (Bot SJ south (7)).

The temperatures on the exposed side of the floor assembly were measured at a number of locations distributed in such a way as to learn, as much as possible, the effect of the fire on the floor assembly. As shown in Figure 17 and Figure 18 (Location of Thermocouples), in the locations at Sections A, B, C, and E, seven thermocouples were installed: 2 at the bottom of two adjacent C-joists, 2 in the cavity at mid-height of the two C-joists, 2 between the subfloor and the two C-joists, and 1 in the cavity at the subfloor at mid-distance between the 2 C-joists. Section D had only 1 thermocouple in the cavity at the subfloor at mid-distance between the 2 C-joists or at mid-height of the interface of the overlapped C-joists.

3.3.7.1 Test UF-04

Figure 30 (a) to Figure 30 (l) show the temperatures of the thermocouples located on the exposed side of the tested floor. For all the locations with 7 thermocouples (A-2, A-7, A-12, B-7, C-1, C-5, C-7, C-9, C-11, C-13, and E-1), in most cases the trend was similar with a sharp increase in temperatures for all the exposed thermocouples in the first 120 s to 180 s. For the thermocouples located at the interface between the top of a C-joist and the subfloor (SF/SJ), the temperature rise occurred in all cases since the steel is highly conductive and the C-joist deflection did not shield the thermocouples for a long time. This is an indication that gaps were forming between the top of the C-joists and the subfloor very early and that the thermocouples were exposed to the hot gases from the fire.

The increase in temperature happened at different times for the different locations. The difference in time between the two SF/SJ (North and South) thermocouples is partly due to the view factor relative to the burning fuel package. In some cases, the bulk of the fuel package was 'positioned' South of the thermocouple grouping. Consequently, the thermocouple at top of the North C-joist experienced a greater heat insult from both the convective and radiative effects from the burning fuel. For the thermocouple groupings with the bulk of the fuel package located to the North, the reverse effect occurred.

Of particular mention is Sections C-9 and C-7 where the temperatures at SF/SJ North (3) and SF/SJ South (5) reached the same or almost the same peak values as the temperatures at the exposed thermocouples in the first 120 s. This is an indication that gaps due to structural movement at the interface of the C-joists and subfloor occurred

much earlier at this location than other locations as it was directly above the mock-up sofa and very close to the wood cribs.

For the exposed thermocouples, the highest peak temperature (a value of about 800ºC) was recorded at sections B-7, C-7, and C-9 (located very close or directly over the burning sofa mock-up and the wood cribs). In some cases, there was a drop in temperature measured by the exposed thermocouples just after 180 s, which may be attributed to the fresh air coming from the open basement window and the opening of the exterior door on the first storey at 180 s. The decrease in temperature was short and then the temperatures started increasing again.

There were cases where there was no obvious drop in the temperature at 160 s (A-1. A-7, A-12, C-1 and E-1). This is because these locations were not in the proximity of the fuel package and thus may have had limited radiative impact from the fuel.

For Section D, the points have the same trend as the exposed thermocouples in Section E.

The temperatures decreased after the extinguishment of the fire was initiated.

NRC·CNRC

a) Thermocouples in cavity A-2

b) Thermocouples in cavity A-7

Figure 30 (a and b). Temperatures at the exposed side for UF-04

NRC·CNRC

c) Thermocouples in cavity A-12

d) Thermocouples in cavity B-7

Figure 30 (c and d). Temperatures at the exposed side for UF-04

NRC·CNRC

e) Thermocouples in cavity C-1

f) Thermocouples in cavity C-5

Figure 30 (e and f). Temperatures at the exposed side for UF-04

NRC·CNRC

g) Thermocouples in cavity C-7

h) Thermocouples in cavity C-9

Figure 30 (g and h). Temperatures at the exposed side for UF-04

NRC·CNRC

i) Thermocouples in cavity C-11

j) Thermocouples in cavity C-13

Figure 30 (i and j). Temperatures at the exposed side for UF-04

k) Thermocouples in cavity D-1, D-2, D-6, D-11 and D-12

l) Thermocouples in cavity E-1

Figure 30 (k and l). Temperatures at the exposed side for UF-04

NRC·CNRC

3.4 Deflection Measurements Results and Structural Performance

Figure 31 shows the 9 deflection measurement 9 points (as well as explained previously; see also Figure 11 for the closest C-joist to the deflection points). The points of measurement were chosen as they were located in the middle of the fire compartment just above the fire load where the impact of the fire on the structural integrity of the floor assembly was anticipated to be the greatest. Some measurement points were aligned with one of the joists, while the other row was positioned between joists.

3.4.1 For Test UF-04

Figure 32 (a) shows the deflections measured in the first row (1, 2, and 3). Up to 120 s, the deflections were very small. After this time, the deflections increased at a relatively moderate rate, reaching a total of 110 mm at 320 s for points No. 1 and No. 2, and 110 mm after 320 s for point No. 3. After these times, all the deflections were constant, which is an indication that the rods had reached their maximum gauge length and were not touching the concrete blocks. So the measured deflections were not the maximum values before floor failure.

Figure 32 (b) shows the deflections measured in the second row (4, 5, and 6). Up to 100 s, the deflections were very small. After this time, the deflections increased at a relatively moderate rate, reaching a total of 120 mm at 280 s for point No. 4, 100 mm at 200 s for point No. 5, and 110 mm after 280 s for point No. 6. After these times, all the deflections were constant, which is an indication that the rods had reached their maximum gauge length and were not touching the concrete blocks. So the measured deflections were not the maximum values before floor failure.

Figure 32 (c) shows the deflections measured in the third row (7, 8, and 9). Up to 100 s, the deflections were very small. After this time, the deflections increased at a relatively moderate rate, reaching a total of 120 mm at 310 s for point No. 7, 120 mm at 300 s for point No. 8, and 130 mm after 310 s for point No. 9. After these times, all the deflections were constant, which is an indication that the rods had reached their maximum gauge length and were not touching the concrete blocks. So the measured deflections were not the maximum values before floor failure. In fact, the failure did not occur until 462 s based on visual observations through the rough window opening in the fire room.

Figure 31. Deflection points measured (all dimensions in mm)

NRC·CNRC

a) Floor Deflection, Row 1

b) Floor Deflection, Row 2

Figure 32 (a and b). Deflection measurements for rows 1, 2 and 3 for UF-04

NRC·CNRC

c) Floor Deflection, Row 3

Figure 32 (c). Deflection measurements for rows 1, 2 and 3 for UF-04

3.5   Flame Penetration Results

Flame penetration through the floor assembly is one of the important aspects of fire performance that is of interest in this project since this is also a failure criterion in standard fire resistance testing. Flames and combustion products penetrating through the subfloor can impact on the time available for evacuation. Any opening(s) created by the flames penetrating the subfloor or excessive deflection would also provide a means for hot fire gases to migrate from the basement fire room to the upper storey(s). As well, the holes would add to the overall weakening of the subfloor. To determine whether there was flame penetration through the floors, both a flame-sensing device and the time-temperature curves on the unexposed side of the floors were used.

3.5.1   For Test UF-04

Figure 33 shows the results of the flame-sensing devices. Three wire meshes were installed on the top of three joints (East, Centre and West) on the unexposed side of the floor as shown in Figure 19 (instrumentation figure). There was a sudden increase in the voltage output of the flame-sensing device when flames penetrated through the floor and struck the wire meshes. As indicated by Figure 33, flame penetration occurred at the centre joint at 180 s, at the west joint at 300 s, and at the east joint at 340 s. This is due to the large deformations that occurred in steel and due to the joint opening created by these deformations.

NRC·CNRC

Figure 33. Results of flame sensors at different joints

3.6 Detection Times

Residential photoelectric and ionization smoke alarms were installed on the ceiling in each bedroom, second storey corridor, first storey and the basement fire compartment. These smoke alarms were powered by batteries and were not interconnected. The ionization smoke alarm was not installed in the basement fire room in order to avoid dealing with radioactive materials in the cleanup of debris after the fire test. Since photoelectric smoke alarms are generally slower in detecting flaming fires than ionization smoke alarms, using the photoelectric smoke alarm in the basement resulted in a more conservative estimate for the activation time for the fire scenario used in the experiment. New smoke alarms were used in each experiment.

Table 2 shows the activation times of the smoke alarms installed in the test facility. The photoelectric smoke alarm in the basement fire compartment took 30 s to activate. It took up to 100 s longer for the smoke alarms in the second storey corridor to activate and up to 220 s longer for the smoke alarms in the closed bedroom to activate. This highlights the importance of having the smoke alarms interconnected to activate simultaneously when one of them detects a fire.

Table 2. Smoke Alarm Activation Times after Ignition (in seconds)

Location	Basement fire room	1st storey		2nd storey corridor		SE bedroom (door closed)		SW bedroom (door open)	
Alarm Type	P	I	P	I	P	I	P	I	P
UF-04	30	65	85	115	130	230	250	160	225

Notes:
1. See section on instrumentation in compartment (Figure 8 to Figure 10)
2. I: ionization, P: photoelectric, SE: South East, SW: South West

NRC·CNRC

3.7   Results of Smoke and Gas Measurements and Tenability Analysis

Fires produce heat, narcotic and irritant gases, and smoke that obscures vision. The temperature and the production of combustion products depend upon the fire characteristics, enclosure geometry and ventilation. The increased temperature and combustion products can, either individually or collectively, create conditions that are potentially untenable for occupants.

Tenability analysis involves examination of the production of heat and toxic products of combustion during the fire tests. It also involves estimation of the potential exposure of occupants, who would have been in the test house, to heat and toxic smoke and of the potential effects as a result of the exposure. The purpose of tenability analysis is to provide an estimation of the time available for escape — the calculated time interval between the time of ignition and the time after which conditions become untenable for an individual occupant.

There are various endpoints for tenability analysis, such as incapacitation, lethality/fatality, etc. For this project, *incapacitation* – a state when people lose the physical ability to take effective action to escape from a fire – was chosen as the endpoint for the tenability analysis related to heat and toxic products of combustion. The time available for escape thus calculated is the interval between the time of ignition and the time after which conditions become incapacitating for an individual occupant.

ISO 13571 and the SFPE Handbook of Fire Protection Engineering provide guidance and methodologies for evaluating the time available for occupants to escape from a fire [15, 16]. These methodologies are used in this report to calculate the time available for escape as an input to the hazard analysis for each fire scenario used in the project. The methodologies include a fractional effective dose (FED) approach to quantify the time at which the accumulated exposure to each fire effluent exceeds a specified threshold criterion for incapacitation. This time then is taken to represent the time available for escape relative to the specified threshold.

The calculated time available for escape depends not only on the time-dependent temperatures, concentrations of combustion gas products and density of smoke in the test house, but also on the characteristics of occupants. The age and health of the occupants (such as body weight and height, lung and respiratory system function, blood volume and hemoglobin concentration, skin, vision, etc.) as well as the degree of activity at the time of exposure have an effect on the consequences of exposure to fire effluents and heat. Since the general population has a wide range of susceptibility to fire effluents and heat, the exposure thresholds for incapacitation can change from subpopulation to subpopulation. Thus, each occupant is likely to have a different time available for escape.

This section of the report does not try to debate what FED criterion should be used as the incapacitation threshold but rather to present the results of the analysis for 2 typical FED values (e.g. FED = 1 and FED = 0.3). The methodology can be used to estimate the time available for escape associated with other FED values, if required.

The time available for escape calculated based on FED =1 represents the time available for a healthy adult of average susceptibility. The distribution of human responses to the fire effluents is unknown but is assumed to be a logarithmic normal distribution [15]. Under this distribution, the time available for escape calculated at FED =1 also represents statistically the time by which 50% of the general population would have been incapacitated but the conditions would still be tenable for the other 50% of the population.

For a more susceptible person, the threshold can be lower and the time available for escape would be shorter than for an average healthy adult. If FED = 0.3 is used as a criterion to determine the time available for escape, it would statistically represent the time by which 11% of the population would have been incapacitated but the conditions would still be tenable for the other 89% of the population [15].

The location of the occupant who would have been in the test house has an effect on the time available for escape. The analysis focused on the fire conditions affecting tenability, as measured on the first and second storeys of the test facility, and the impact on any occupant assumed to be present on the upper storeys of the test house at the time of ignition. In real fire situations, the occupant would move through different locations during egress. Therefore, the time to incapacitation would be in-between the times calculated for different locations. The conditions in the basement fire room would not be survivable once flashover occurred.

The methodology used does not address quantitatively any interaction (combined effects) between heat, combustion gas products and smoke obscuration. Each component is treated as acting independently on the occupants to create incapacitating conditions and the time available for escape is the shortest of the times estimated from consideration of exposure to combustion gas products, heat and visual obscuration.

It is necessary to recognize that 2 types of uncertainty exist in the tenability analysis: the uncertainties associated with the experimental data and the uncertainties associated with the equations used for FED calculations. Fortunately, with the fast-growing fire used in the project, the resulting uncertainty in the estimated time available for escape is much smaller than the uncertainty in the calculated FED due to their non-linear relationship. More details are provided in the following sections.

3.7.1   Exposure to Toxic Gases

Exposure to toxic products of combustion from fires has been a major cause of death and injury in many fire incidents. Understanding the toxic effect of the smoke products and predicting the exposure time necessary to cause incapacitation are complex problems.

In regards to the fuel package used in this study, with the combined flaming combustion of polyurethane foam and wood cribs, the primary gas products were toxic carbon monoxide (CO) and asphyxiant carbon dioxide (CO_2) in a vitiated oxygen (O_2) environment. Given the amount of polyurethane foam in the fuel package and the volume of the test house, hydrogen cyanide (HCN) produced from the combustion of polyurethane foam would not reach a concentration of concern for occupant life safety. A literature review by Beyler concluded that exposure to products of flaming combustion

NRC·CNRC

of flexible polyurethane foam would result in CO levels in the blood of test animals generally consistent with simple CO exposure, despite the toxicological role of HCN [17]. The fuel package contained no chemical components that would produce acid halides in the combustion gases. In this report, the analysis involved CO and CO_2 and oxygen vitiation only.

Table 3 shows the maximum CO and CO_2 concentrations and the minimum O_2 concentrations for Test UF-04. Figure 34 to Figure 36 (figures commence on page 62) show the CO, CO_2 and O_2 concentration-time profiles measured during Test UF-04. Note that some gas analyzers had upper limits of 10% for CO_2 measurements and/or 1% for CO measurements and that the CO_2 concentration profile above the 10% measurement range for the first storey at the 1.5 m height was calculated using the measured O_2 and CO concentrations ($CO_2\% = 20.9\% - O_2\% - \frac{1}{2} CO\%$) (see Figure 36). The gases were well mixed in the test house during the test.

The SFPE Handbook of Fire Protection Engineering contains information on the tenability limits for incapacitation or death after a 5-min exposure [16], shown in Table 4, which indicate the test results that need to be analyzed. In the following sections, tenability due to each gas is first analyzed independently; the interaction between gases is then considered.

Table 3. Maximum CO and CO_2 Concentrations and Minimum O_2 Concentration (%)

		Test UF-04
2nd storey 1.5 m high	CO	>1.0
	CO_2	>10.0
	O_2	2.3
2nd storey 0.9 m high	CO	1.6
	CO_2	17.0
	O_2	2.7
1st storey 1.5 m high	CO	2.1
	CO_2	>10.0 17 *
	O_2	1.9
1st storey 0.9 m high	CO	>1.0
	CO_2	>10.0
	O_2	1.9

Notes:
1. ">" indicating the concentration beyond the measurement range of the gas analyzer;
2. All concentrations before the structural failure;
3. *calculated: $CO_2\% = 20.9\% - O_2\% - \frac{1}{2} CO\%$.

Table 4. Tenability Limits for Incapacitation or Death after 5-min Exposure [16]

Gas	Incapacitation	Death
CO	6000 – 8000 ppm (0.6 – 0.8%)	12,000 – 16,000 ppm (1.2 – 1.6%)
Low O_2	10 – 13%	< 5%
CO_2	7 – 8%	> 10%

NRC·CNRC

3.7.1.1 Exposure to O_2 vitiation

Fires consume oxygen and create a low oxygen atmosphere. Past human experiments in an oxygen-depleted atmosphere indicated that most people could tolerate a 15% O_2 atmosphere [16]. Healthy individuals could also tolerate a 12% O_2 level for a short period (<5 min) [18]. When oxygen diminished to below 10%, unconsciousness could occur rapidly. For healthy adults, the following equation was derived from the experiments with human subjects [16] and can be used to predict the time, t_{in,O_2} (minute), to loss of consciousness due to lack of oxygen alone.

$$t_{in,O_2} = \exp[8.13 - 0.54(20.9 - \%O_2)]$$

With the changing O_2 concentration, the fractional effective dose approach has to be used in the analysis. The incapacitation dose for oxygen vitiation can be expressed by $(20.9 - \%O_2) \times t_{in,O_2}$. The fractional effective dose is the accumulation of the ratio of the actual exposure dose $(20.9 - \%O_2) \times \Delta t$ and the incapacitation dose at each discrete increment of time:

$$F_{in,O_2} = \sum_{t1}^{t2} \frac{(20.9 - \%O_2) \cdot \Delta t}{(20.9 - \%O_2) \cdot t_{in,CO_2}} = \sum_{t1}^{t2} \frac{\Delta t}{\exp[8.13 - 0.54(20.9 - \%O_2)]}$$

where Δt (minute) is the discrete increment of time, i.e. the time interval for data sampling. Table 5 shows the calculated times for the fractional effective dose reaching 0.3 and 1.0 for exposure to O_2 vitiation alone.

In Test UF-04 (see Figure 35), the O_2 concentration on both the first and second storeys dropped to below 10% in 250 s and to 3% at 460 s after ignition. The O_2 vitiation alone would cause incapacitation after 335-345 s (1st storey-2nd storey) using $F_{in,O_2} = 1$ as a criterion, or after 295-305 s (1st storey-2nd storey) using $F_{in,O_2} = 0.3$.

3.7.1.2 Exposure to CO_2

CO_2 is not toxic at concentrations of up to 5%. Above 7%, CO_2 becomes an asphyxiant gas; the danger of loss of consciousness of an exposed person increases. Loss of consciousness could occur in approximately 2 minutes at 10% CO_2, for example. The following equation can be used to predict the time, t_{in,CO_2} (minute), to loss of consciousness due to the CO_2 asphyxiant effect [16]:

$$t_{in,CO_2} = \exp(6.1623 - 0.5189 \cdot \%CO_2)$$

With the changing CO_2 concentration, the fractional effective dose approach has to be used. The incapacitation dose for CO_2 exposure can be expressed by $\%CO_2 \times t_{in,CO_2}$ above which loss of consciousness would occur for people of average susceptibility. At each discrete increment of time, the increment of the fractional effective dose was calculated as the actual exposure dose (CO_2 concentration $\times$ time

NRC·CNRC

increment) divided by the incapacitation dose. The fractional effective dose values expressed in Table 5 are the accumulation of this ratio of each time increment:

$$F_{in,CO_2} = \sum_{t1}^{t2} \frac{\%CO_2 \cdot \Delta t}{\%CO_2 \cdot t_{in,CO_2}} = \sum_{t1}^{t2} \frac{\Delta t}{\exp(6.1623 - 0.5189 \cdot \%CO_2)}$$

In Test UF-04 (see Figure 36), the CO_2 concentration exceeded 10% (measurement range limit of the gas analyzers) in 250 s. Note that the CO_2 concentration profile above the 10% measurement range was calculated for the first storey at the 1.5 m height using the measured O_2 and CO concentrations ($CO_2\%=20.9\%$ - $O_2\%$ - ½ $CO\%$). The increased concentration of CO_2 alone would cause incapacitation after 285-310 s (1st storey-2nd storey) using F_{in,CO_2} = 1 as a criterion, and after 260-280 s (1st storey-2nd storey) using F_{in,CO_2} = 0.3.

3.7.1.3 Exposure to CO

CO is known to be the most important toxicant of the fire gases. The lowest CO concentration in air that has been reported to cause human death is 5,000 ppm for a 5 min exposure [19]. The toxic effect of CO is due to its affinity with the hemoglobin in human blood to form carboxyhemoglobin (COHb), which reduces the transport of oxygen in the blood to various parts of the body. When COHb in the blood increases to a threshold concentration, loss of consciousness or death may occur. The time for the toxic effect to occur depends on the uptake rate of CO into the blood of a victim and the threshold COHb concentration for that victim.

The CO uptake rate is determined by the difference between the CO concentration inhaled and that already in the body, and varies with the breathing rate, the degree of activity, the lung function, the body size, the blood volume and hemoglobin concentration of the victim and the exposure duration. The complexity of the CO uptake is described by the theoretical Coburn-Forster-Kane (CFK) equation, which takes account of a wide range of variables to predict the COHb concentration [20]. For high-concentration and short-duration exposures such as the fire scenarios used in the FPH tests, one can use a simpler equation that was derived from human exposure experiments with healthy adults [16, 21]:

$$\%COHb = 3.317 \times 10^{-5} [CO]^{1.036} RMV \cdot t$$

where *[CO]* is the inhaled carbon monoxide concentration in *parts per million*, *RMV* (respiratory minute volume) is the volume of air breathed in *litres per minute*, and *t* is the exposure duration in *minutes*. This equation gives equally good predictions as the CFK equation for average healthy adults. Since the CO concentration in the experiments varied with time, %COHb was calculated as a summation of the CO uptake at each discrete time step:

$$\%COHb = \sum_{t_0}^{t} 3.317 \times 10^{-5} [CO]^{1.036} RMV \cdot \Delta t$$

For an average adult, the normal breathing rate is 20 L/min with light activity. The breathing rate is affected by the presence of CO_2 in a fire situation. In the concentration range of 2 to 6%, CO_2 can stimulate breathing. A CO_2-induced hyperventilation factor, VCO_2, for breathing can be estimated using [16]:

$$VCO_2 = \exp(\frac{\%CO_2}{5})$$

The hyperventilation increases the uptake rate of other toxic gases, such as CO, from the fire. This effect should be considered when CO_2 concentration is above 2%. The presence of 5% CO_2 could triple the normal breathing rate, for example. Considering the CO_2-induced hyperventilation in a fire situation, the breathing rate would be

$$RMV = 20 \cdot \exp(\frac{\%CO_2}{5})$$

For the same individual, the CO uptake rate changes if the breathing rate changes, which also depends on the degree of activity of that individual. The CO uptake rate varies from person to person for a given smoke atmosphere.

The COHb incapacitating concentration at which loss of consciousness may occur is in the range of 25-40% depending on the degree of activity of the occupant among other variables [16, 22]. The threshold of 40% is more appropriate for those at rest and 30% for those engaged in light activity [16]. Certain susceptible populations may be incapacitated at lower COHb concentrations.

With the rate of CO uptake and the likely incapacitating concentration of COHb, time to incapacitation due to CO exposure can be predicted. For those engaged in light activity, the fractional effective dose for incapacitation due to the CO uptake can be expressed as the COHb concentration in the blood divided by the incapacitating COHb concentration

$$F_{in,CO} = \frac{\%COHb}{30} = 2.2113 \times 10^{-5} \sum_{t_0}^{t} [CO]^{1.036} \Delta t \cdot \exp(\frac{\%CO_2}{5})$$

Alternatively, the fractional effective dose for incapacitation due to CO can also be calculated using the approach given in ISO TS 13571 for short exposure to CO at high concentrations [15]:

$$F_{in,CO} = \sum_{t1}^{t2} \frac{[CO] \cdot \Delta t}{35000} \exp(\frac{\%CO_2}{5})$$

where the incapacitation dose is 35000 ppm·min, which is consistent with the tenability limits of 6000 to 8000 ppm for incapacitation for 5-min exposure given in the SFPE Handbook of Fire Protection Engineering [16]. For the FPH tests, the difference between the incapacitation times predicted using these two equations is relatively small.

NRC·CNRC

The time to incapacitation determined using $F_{in,CO} = 1$ as a criterion represents the time available for escape for healthy adults of average susceptibility. For more susceptible people, the exposure thresholds could be lower. The CO uptake and the COHb increase are known to be faster in small children than in adults [23]. Therefore, the incapacitation time for small children or a more susceptible subpopulation would be shorter than for average healthy adults. These can be addressed, to a certain degree, by using $F_{in,CO} = 0.3$ as a criterion to determine the incapacitation time. Table 5 shows the calculated times for the fractional effective dose reaching 0.3 and 1.0. Calculation for the CO fractional effective dose was done with and without the CO_2 hyperventilation factor $exp(\%CO_2/5)$.

In Test UF-04 (see Figure 34), the maximum CO concentration prior to failure of the floor assembly was 21000 ppm at 460 s. The increased concentration of CO alone would cause incapacitation after 295-305 s (1st storey-2nd storey) using $F_{in,CO} = 0.3$ as a criterion, and after 405-425 s (1st storey-2nd storey) using $F_{in,CO} = 1.0$. With CO_2-induced hyperventilation, these times were reduced to 220-245 s (1st storey-2nd storey) for $F_{in,CO} = 0.3$ and 260-280 s (1st storey-2nd storey) for $F_{in,CO} = 1.0$.

Table 5. Time (in seconds) to the Specified Fractional Effective Dose for Exposure to O_2 Vitiation, CO_2 and CO

	Test UF-04	
Fractional Effective Dose	**FED = 0.3**	**FED = 1.0**
CO alone – 1st storey	295	405
CO with CO_2 hyperventilation – 1st storey	220	260
Low O_2 hypoxia – 1st storey	295	335
CO alone – 2nd storey corridor	305	425
CO with CO_2 hyperventilation – 2nd storey corridor	245	280
Low O_2 hypoxia – 2nd storey corridor	305	345
High CO_2 hypercapnia – 1st storey	260	285
High CO_2 hypercapnia – 2nd storey corridor	280	310

Note:
Based on concentrations at 1.5 m height

3.7.1.4 Interaction of CO, CO_2 and O_2 vitiation

Interactions between these gases and their combined effect are not well understood. The asphyxiant effect of CO_2 is generally treated as being independent of other gases; the effect of O_2 vitiation (low oxygen hypoxia) is generally treated as being additive with the toxic effect of CO [16]. The effect of the smoke gases is determined by F_{in,CO_2} or $(F_{in,CO} + F_{in,O_2})$, whichever is larger (with $F_{in,CO}$ including the effect of CO_2-induced hyperventilation).

Table 6 shows examples of this treatment. The calculation shows that the O_2 vitiation did not add much to the effect at the time when CO was capable of producing incapacitation. CO was the most important toxicant of the smoke gases; increased CO

NRC·CNRC

uptake by CO_2-induced hyperventilation was the most important interaction. Therefore, the exposure to CO with CO_2-induced hyperventilation determined the incapacitation time for the gases analyzed. Assuming the rate of CO uptake remains unchanged, the time required from the incapacitation dose to the lethal dose for an average adult is estimated to be within 1 minute under the conditions of Test UF-04.

A recent paper by Gann includes an analysis of incapacitation by exposure to CO alone for a susceptible subpopulation such as people with coronary artery disease or small children; incapacitation could occur at an FED range of 0.14-0.21 (CO alone) [24]. As shown in Table 6, when the FED due to CO exposure with CO_2 hyperventilation reached 0.3, the FED due to CO exposure alone was very close to this range. This shows consistency in the estimation of time to incapacitation.

Table 6. FED due to CO, CO_2, O_2 Vitiation at Specified Time

	Test UF-04 1st storey SW quadrant 1.5 m height		Test UF-04 2nd storey corridor 1.5 m height	
Time	**220 s**	**260 s**	**245 s**	**280 s**
CO alone	0.12	0.2	0.1	0.2
CO $\times$ CO_2 hyperventilation	0.32	1.0	0.3	1.0
Low O_2 hypoxia	0.006	0.05	0.02	0.1
CO $\times$ CO_2 hyperventilation + low O_2 hypoxia	0.33	1.05	0.3	1.1
High CO_2 hypercapnia	0.03	0.3	0.04	0.3

For exposure to the gases, each calculation for estimating incapacitation in this section was associated with a particular position where the concentrations were measured – each calculated time applies to an occupant who would stay at that particular location. In real fire situations, the occupant would move through different locations during egress. Therefore, the time to incapacitation would be in-between the times calculated for different locations.

3.7.2 Exposure to Heat

Convected heat is the most important source of heat exposure for occupants in the first and second storeys. Figure 23 to Figure 24 and Figure 26 to Figure 27 show the temperature-time profiles measured on the two upper storeys during the tests. The temperatures at the 1.4 m height above the floor were used for the analysis of convected heat exposure.

The rate of convective heat transfer from hot gases to the skin depends on temperature, ventilation, humidity of the enclosure and clothing over the skin [16]. The tolerable time of exposure to convected heat is 15 min for dry air of 100°C or saturated air of 80°C. For hot air at temperatures above 120°C and with water vapour of less than 10%, pain and skin burns would be likely to occur in minutes; assuming unclothed or lightly clothed subjects, the time to incapacitation due to exposure to convected heat, $t_{in,conv}$ *(minutes)*, can be estimated for a constant temperature T $(°C)$ using [15, 16]:

NRC·CNRC

$$t_{in,conv} = 5 \times 10^7 T^{-3.4}$$

Since the temperatures in the FPH experiments were changing, the exposure was estimated using the fractional effective dose analogy at each discrete increment of time, Δt *(minutes)*:

$$\frac{\Delta t}{t_{in,conv}} = \frac{T^{3.4}}{5 \times 10^7} \Delta t$$

When the temperature is increasing or stable, the fractional effective dose for incapacitation due to the convected heat exposure can be calculated using the following equation:

$$F_{in,heat} = \sum_{t1}^{t2} \frac{\Delta t}{t_{in,conv}} = \sum_{t1}^{t2} \frac{T^{3.4}}{5 \times 10^7} \Delta t$$

The calculated time to incapacitation due to the convected heat exposure is given in Table 7. Radiant heat is important when the hot smoke layer is over 200°C, which corresponds to the threshold radiant heat flux of 2.5 kW·m^{-2} required to produce second degree burning of skin [25]. The calculation indicated that the convected heat exposure would result in incapacitation before the radiant heat began to play a major role on the first and second storeys.

Each calculation was associated with a particular position where the temperature was measured; in other words, each calculated time applies to an occupant who would stay at the location of a particular thermocouple tree. In real fire situations, the occupant would move through different locations during egress. Therefore, the time to incapacitation would be in-between the times calculated for different locations.

For Test UF-04, the convective heat exposure alone would produce incapacitation, but the time depended on the location in the test house. In the corridor on the second storey, the incapacitation time would be after 250 s and 290 s for $F_{in,heat}$=0.3 and $F_{in,heat}$= 1, respectively. In the open bedroom, the incapacitation time would be after 325 s and 460 s for $F_{in,heat}$= 0.3 and $F_{in,heat}$= 1, respectively. Heat exposure would not contribute to incapacitation in the closed bedroom ($F_{in,heat}$<0.01). On the first storey, the incapacitation time would be after 207-216 s using $F_{in,heat}$= 0.3 as a criterion, and 215-229 s using $F_{in,heat}$= 1.

Table 7. Time (in seconds) to the Specified FED for Exposure to Convected Heat

	Test UF-04	
Fractional Effective Dose	**FED = 0.3**	**FED = 1.0**
1st storey SE quadrant	210	215
1st storey SW quadrant	207	215
1st storey NE quadrant	215	227
1st storey NW quadrant	216	229
2nd storey corridor	250	290
2nd storey open bedroom	325	460
2nd storey closed bedroom	n.r. (FED < 0.01)	n.r. (FED < 0.01)

Notes:
1. Based on temperatures at 1.4 m height;
2. n.r. – not reached.

3.7.3 Visual Obscuration by Smoke

Visual obscuration by the optically dense smoke tended to be the first hazard to arise that could impede evacuation by the occupants. Although visual obscuration would not directly cause incapacitation, it would cause delays in movement by the occupants and thus prolong exposure of occupants to other hazards.   In this report, the smoke obscuration is expressed as the optical density per meter (OD in m^{-1}):

$$OD = \frac{1}{L}\log_{10}\left(\frac{I_0}{I}\right)$$

where I_0 is the intensity of the incident light, I is the intensity of the light transmitted through the path length, L (m), of the smoke. The optical density is related to the extinction coefficient (k in m^{-1}) by $OD = k/2.303$.

Studies by Jin indicated that the optical density of smoke and visibility through smoke are related (the visibility is proportional to the reciprocal of the OD for non-irritating smoke, for example) [26]. Various threshold OD values related to the loss of visibility have been suggested for small buildings with occupants familiar with the egress route. The limiting OD value was suggested to be 0.5 m^{-1} for non-irritating smoke and 0.2 m^{-1} for irritating smoke [16,26]. A limiting OD value of 0.5 m^{-1} was also set by Babrauskas using the results of full-scale burns of upholstered chairs and mattresses [22,27]. A recent home smoke alarm study used an OD of 0.25 m^{-1} as the tenability limit for smoke obscuration [28]. In ISO 13571[15], the minimum visible brightness difference between an object and a background is used to estimate the smoke obscuration limit at which occupants cannot see their hands in front of their faces (a distance of 0.5 m or less). These calculations indicate that occupants cannot see their hands in front of their faces and become disoriented at an optical density of 3.4 m^{-1}. For an occupant whose vision is impaired, this can happen at an optical density of 2 m^{-1} or less.

Video records were also analyzed for visual obscuration. The video images became completely obscure when the optical density was approaching 2 m^{-1}. Note that there were at least 2 halogen lamps (2 x 500 Watts) providing lighting in the view direction of

NRC·CNRC

each video camera on the first and second storey. This lighting condition was much better than that in a real house.

In this report, a tenability limit for optical density is set at $OD_{Limit} = 2$ m^{-1}, recognizing that this limit could be lower for people with impaired vision. The time to untenable smoke obscuration is the moment when the optical density reaches this limit. Times to reach other smoke levels are also provided for discussion.

Figure 37 shows the optical density-time profiles measured on the first and second storeys. The times to reach various optical density levels at different locations for this series of the tests are listed in Table 8. It must be pointed out that the smoke density meters used for the first storey had a narrower range of signal output (0.15 to 0 V) while the smoke density meters used for the second storey had a wider working range (1 to 0 V). The starting voltage (0.15 or 1 V when there was no smoke) decreased due to smoke residue left over from the preceding tests on the light source and the detector inside the meters. This reduced the working range particularly for the smoke density meters used for the first storey, which became saturated at a lower OD level than the meters used for the second storey. The smoke density meters used for the first storey were not able to measure the smoke obscuration of $OD = 2$ m^{-1} and beyond. The analysis of video records indicated that by the time when $OD = 2$ m^{-1} was reached in the corridor on the second storey, there was complete smoke obscuration in the test house.

In a separate study, fire scenario (FS) tests were conducted in the test facility with the ceiling of the basement fire room lined with two layers of non-combustible cement board (no structural floor was installed above the fire room). Ventilation and door openings in Test FS-1 were the identical to those in Test UF-04. Information about Test FS-1 can be found in data compilation and analysis reports [6, 29].

In Test UF-04, the increase in the optical density at each measurement location was quite fast. The times to reach various optical density levels of interest were very similar to the fire scenario Test FS-1. The combustion of the polyurethane foam produced sufficient smoke for conditions to reach the smoke obscuration limit. Both the optical density measurements and video records indicate that complete visual obscuration occurred around 200 s in the test house.

Psychological effects of smoke on occupants may accelerate the loss of visibility [26]. Possible reduction of time to untenable smoke level due to psychological effect is not addressed in this report.

Table 8. Time (in seconds) to the Specified Smoke Optical Density

	Test UF-04			
OD (m^{-1}) =	0.25	0.50	1.0	2.0
1st storey SW quadrant 1.5 m height	115	145	160	n.a.
1st storey SW quadrant 0.9 m height	145	180	190	n.a.
2nd storey corridor 1.5 m height	145	170	180	195
2nd storey corridor 0.9 m height	160	180	190	205

Note:
1. n.a. – not available due to limited measurement range of the smoke meters used for the first storey.

NRC·CNRC

3.7.4 Summary of Estimation of Time to Incapacitation

Tenability was analyzed independently for gas exposure, heat exposure and smoke obscuration to estimate the time available for escape, using incapacitation as the endpoint. The combined incapacitating effect as a result of simultaneous exposure to the combustion gases, heat and smoke obscuration is not well understood. Table 9 summarizes the estimated times to the onset of untenable conditions, where each value is the shortest time among each set of values from Table 5, Table 7 and Table 8.

The uncertainty in the calculation of the FED is estimated to be ±25% for the heat exposure and ±40% for the CO exposure (with CO_2 induced hyperventilation) [15]. With the fast-growing fire used in the FPH project, the resulting uncertainty in the estimated time is much smaller than the uncertainty in the calculated FED due to the non-linear relationship. The uncertainty in the timing of the optical density measurement is ±5 s. Table 9 lists the uncertainty in the estimated time.

Table 9. Summary of Estimation of Time to Specified FED and OD (in seconds)

Test	OD = 2 m^{-1}	FED = 0.3		FED = 1	
	2nd storey	1st storey	2nd storey	1st storey	2nd storey
Tests with open basement doorway					
FS-1	190±5	*245±15*	*260±15*	*290±20*	*325±30*
UF-04	195±5	**207±2**	*245±10*	**215±3**	*280±20*

Notes:
1. Values determined using the measurements at 1.5 m height (for gas concentrations and OD) or 1.4 m height (for temperatures);
2. The number with the *Italic* font represents the calculated time for reaching the CO incapacitation dose, while the number with the bold Arial font represents the calculated time for reaching the heat incapacitation dose, whichever occurred first.

Smoke obscuration was the first hazard to arise. Although smoke obscuration would not directly cause incapacitation, it could impede evacuation and prolong exposure of occupants to other hazards. In Test UF-04, the time to reach various optical density levels of interest was very similar to that of Test FS-1 and the combustion of polyurethane foam was mainly responsible for reaching the smoke obscuration limit. It must be pointed out that people with impaired vision could become disoriented at a lower optical density.

Because of the variation in susceptibility to heat and/or gas exposure, the time to untenable conditions was not a single value. The times corresponding to FED = 0.3 and FED = 1 in Table 9 represent this variation to a certain extent. There was also a slight variation of the corresponding time on the 2 different storeys, which is reflected by the time range for each FED in Table 9. It should be pointed out that in Test UF-04, the heat exposure and the CO exposure (with hyperventilation) would cause incapacitation at a similar time, independently.

NRC·CNRC

For the closed bedroom, only heat exposure could be estimated. Based on the temperature measurements and the heat exposure calculation, the conditions in the closed bedroom on the second storey would not reach untenable conditions associated with FED = 0.3 or 1.

The analysis so far addressed a potential exposure that started at the time of ignition, which applies to occupants who would have been in the open spaces of the house.

Further analysis was also conducted for exposure starting at times later than ignition. This further analysis is important for occupants who would have been in the closed bedroom but tried to open the bedroom door to escape through the normal routes.

Figure 38 shows the time remaining to incapacitation calculated from the convected heat and hyperventilated CO exposure for people of average susceptibility (FED=1) and for more susceptible occupants (FED=0.3) as a function of onset of exposure. Again, this calculation was associated with particular positions where the concentrations or temperatures were measured (each calculated time applies to an occupant who would have stayed at that particular location). The actual time to incapacitation would be in between the times calculated for different locations since an occupant would have moved through different locations during egress.
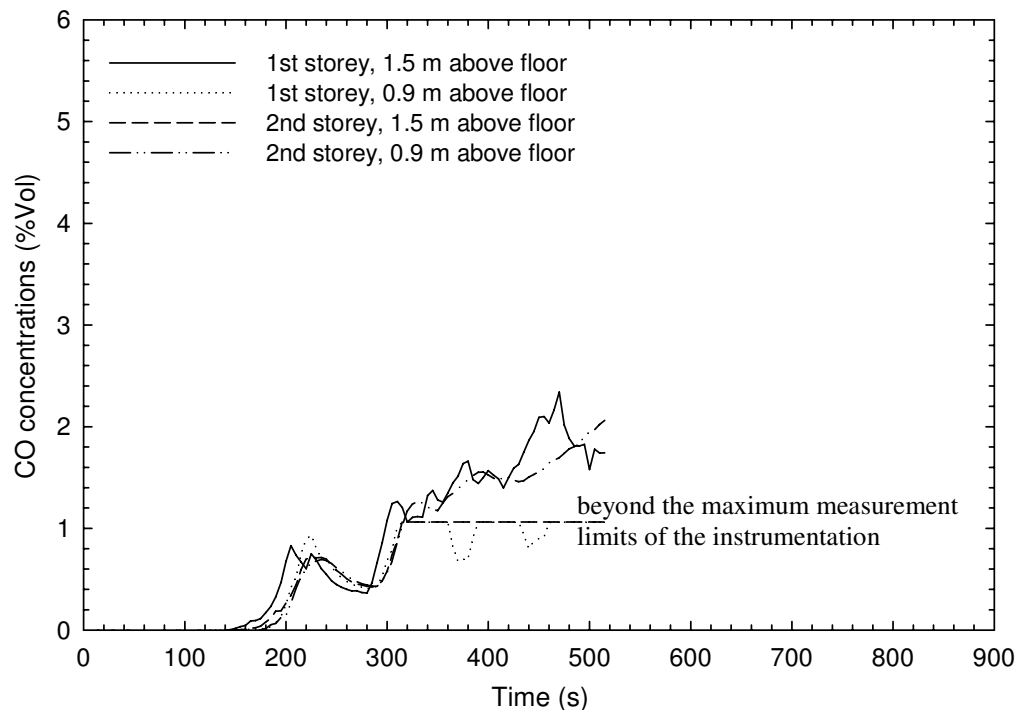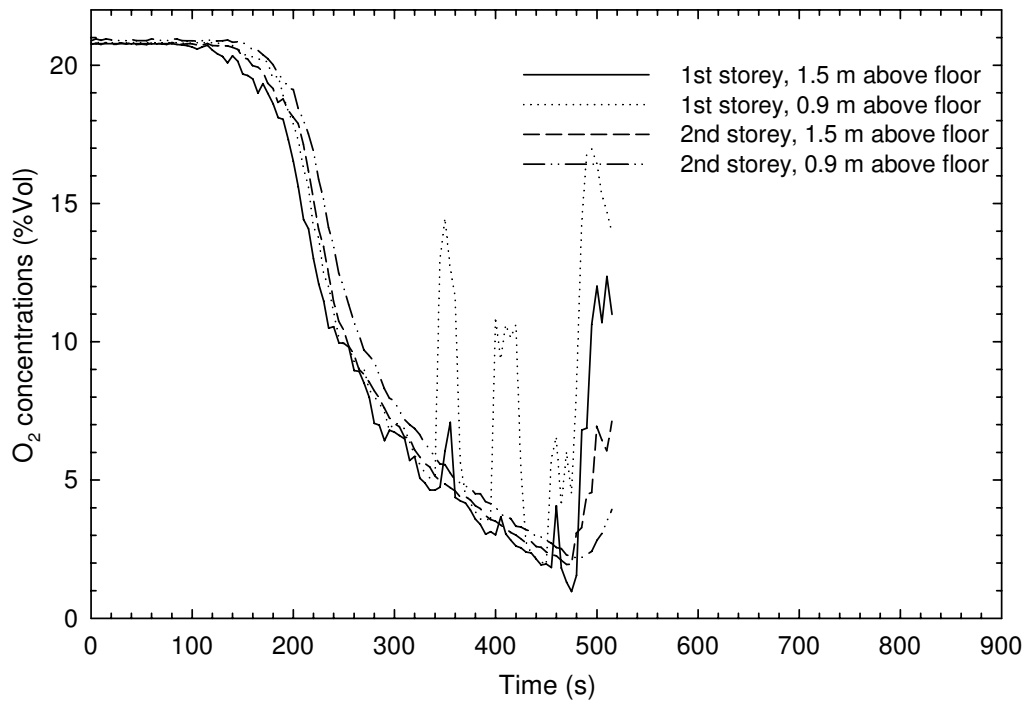

Figure 34. CO measurements for Test UF-04
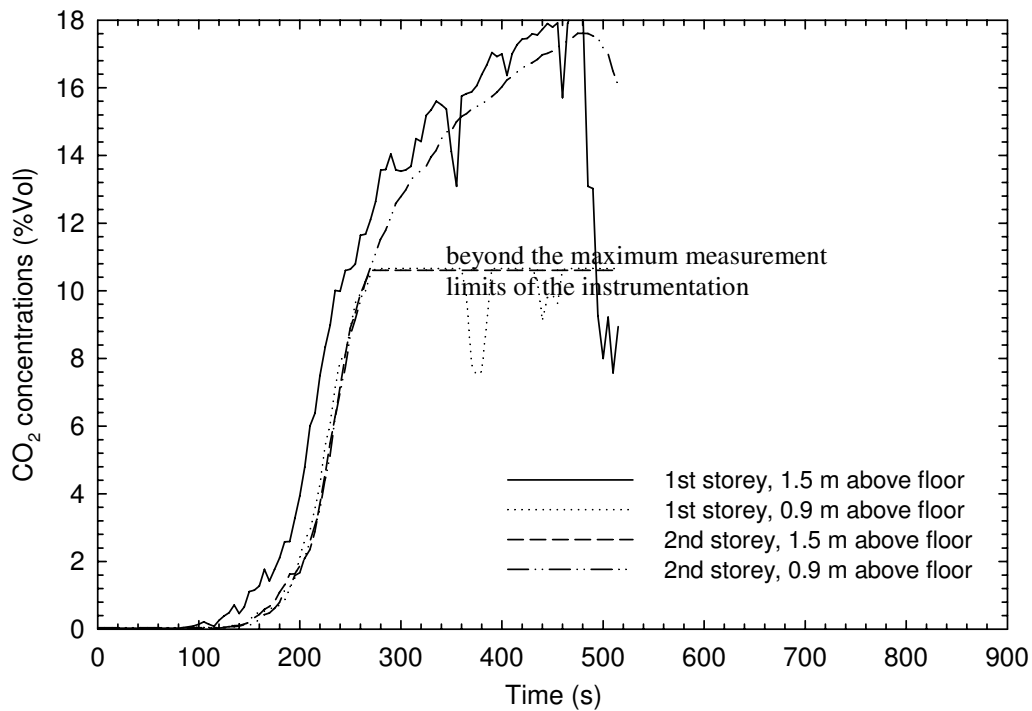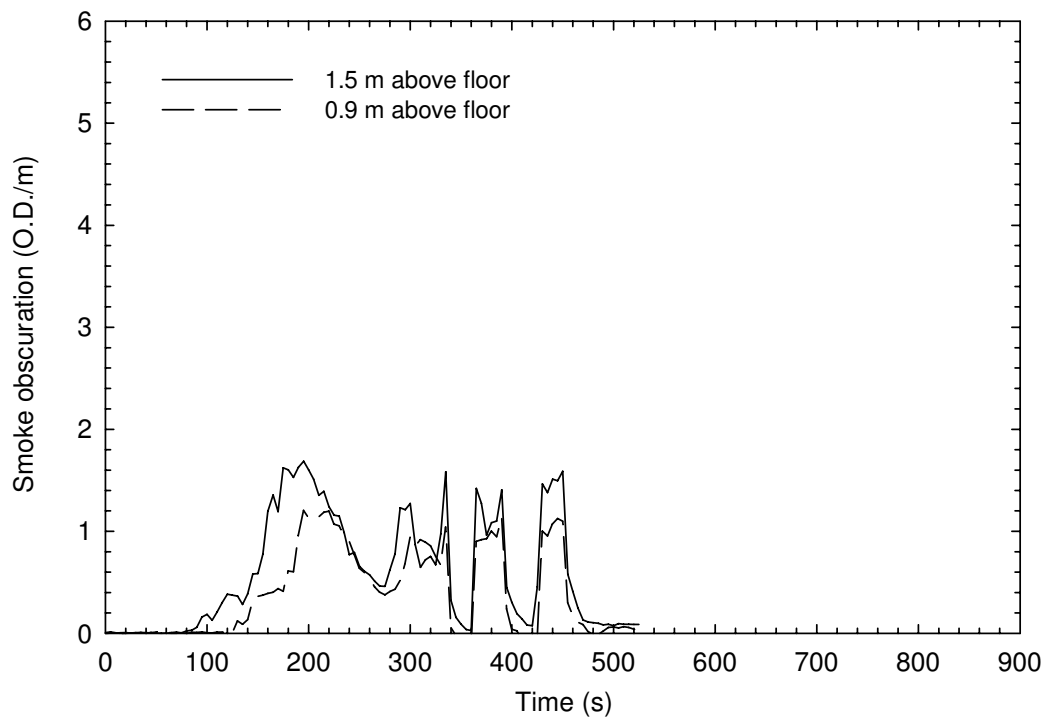
Figure 35. O$_2$ measurements for Test UF-04
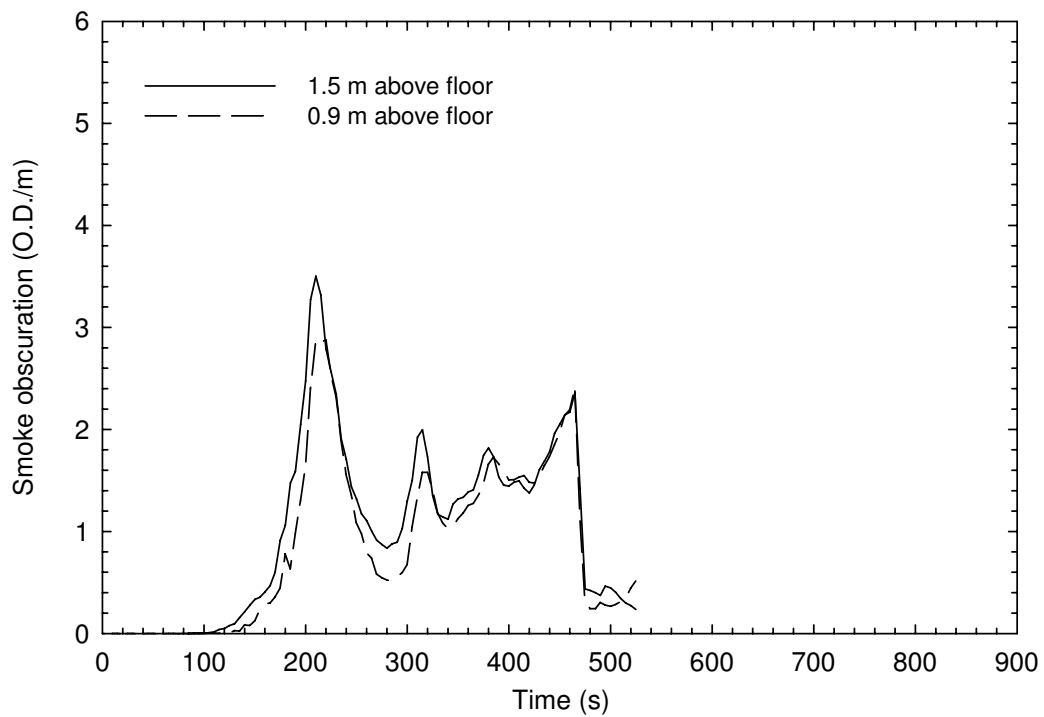

Figure 36. CO$_2$ measurements for Test UF-04

NRC·CNRC

a) Smokemeters - 1st storey SW quadrant

b) Smokemeters - 2nd storey corridor

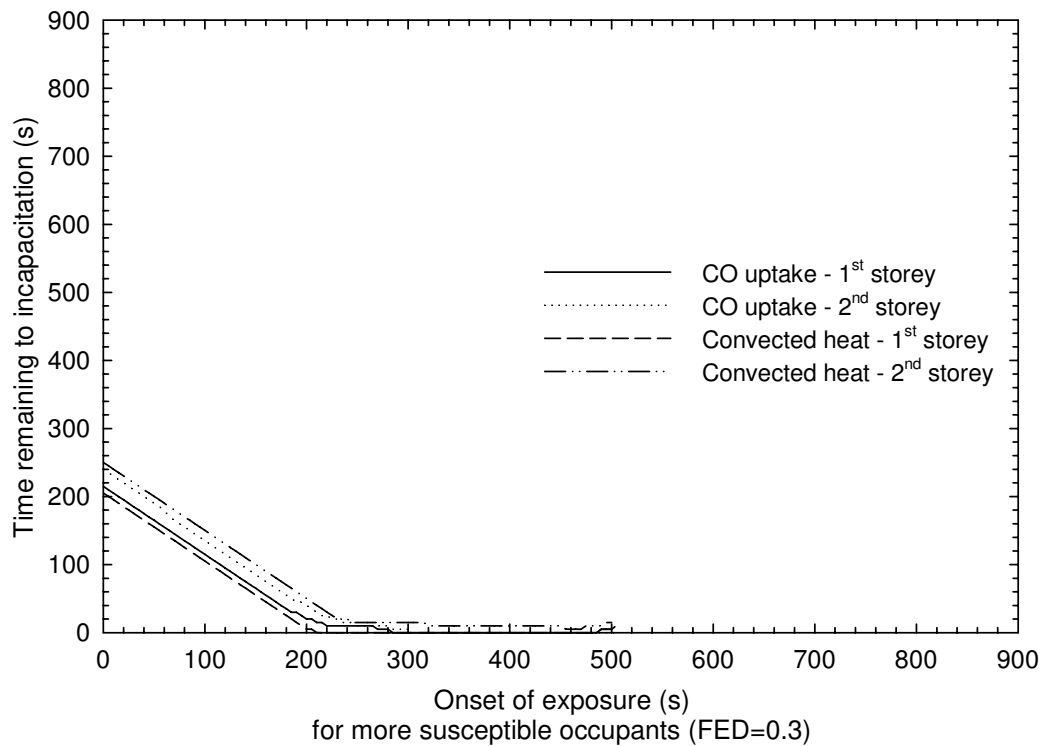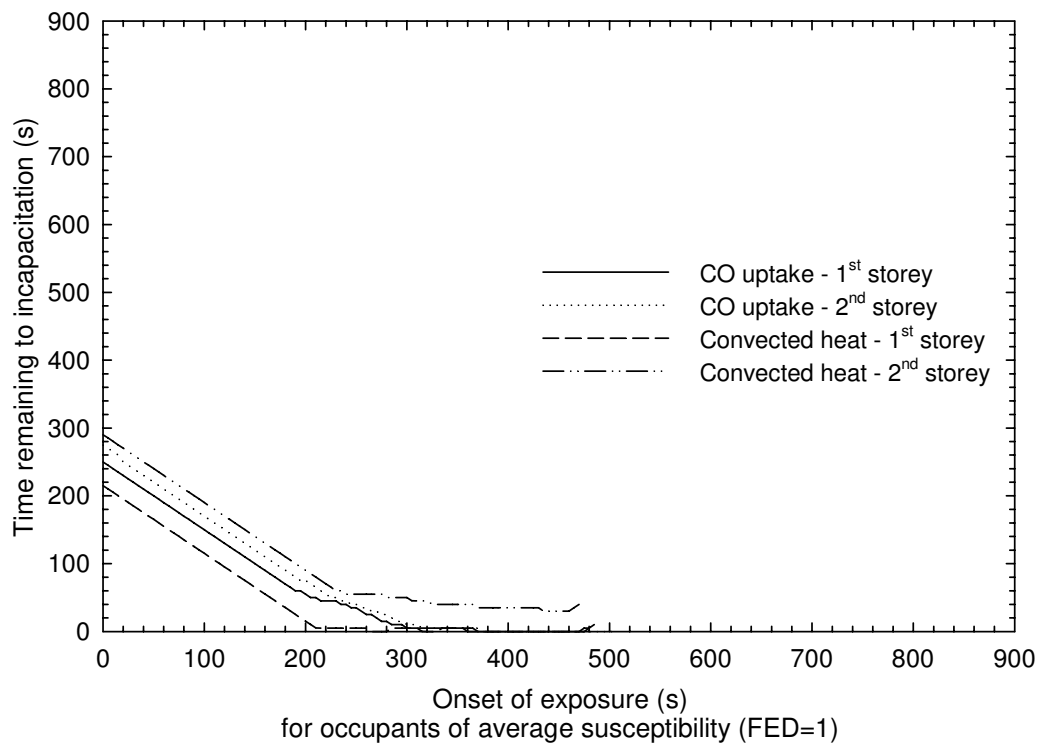**Figure 37. Optical density measurements for Test UF-04**

NRC·CNRC

Figure 38. Time remaining to incapacitation versus onset of exposure for Test UF-04 (ignition at time zero)

3.8   The Sequence of Events

Figure 39 shows the chronological sequence of the fire events in Test UF-04. The smoke alarm (photoelectric) located in the basement detected the fire quickly at 30 s. Interconnecting all of the smoke alarms in the house would help ensure an early fire alert.

The basement window was opened after it reached 300°C at 120 s in Test UF-04. The exterior door on the first storey was opened at 180 s.

The timing for onset of potentially untenable conditions includes those for the complete smoke obscuration (OD $\geq$ 2 m^{-1}) and for exposure to heat and narcotic gases for susceptible (FED =0.3) and average (FED=1.0) occupants (see Section 3.7 for detailed discussions). The untenable conditions were reached before the structural failure of the floor assembly. The time after which the floor structure would be no longer usable for egress (462 s for UF-04) was based on the shortest time to reach the maximum deflection. The test was terminated after the floor failure.

Initiation of fire (0 s)

Smoke alarm activation (30 s)

Onset of untenable conditions
OD $\geq$ 2 m^{-1} (195 s)

FED = 0.3~1.0 (207~280 s)

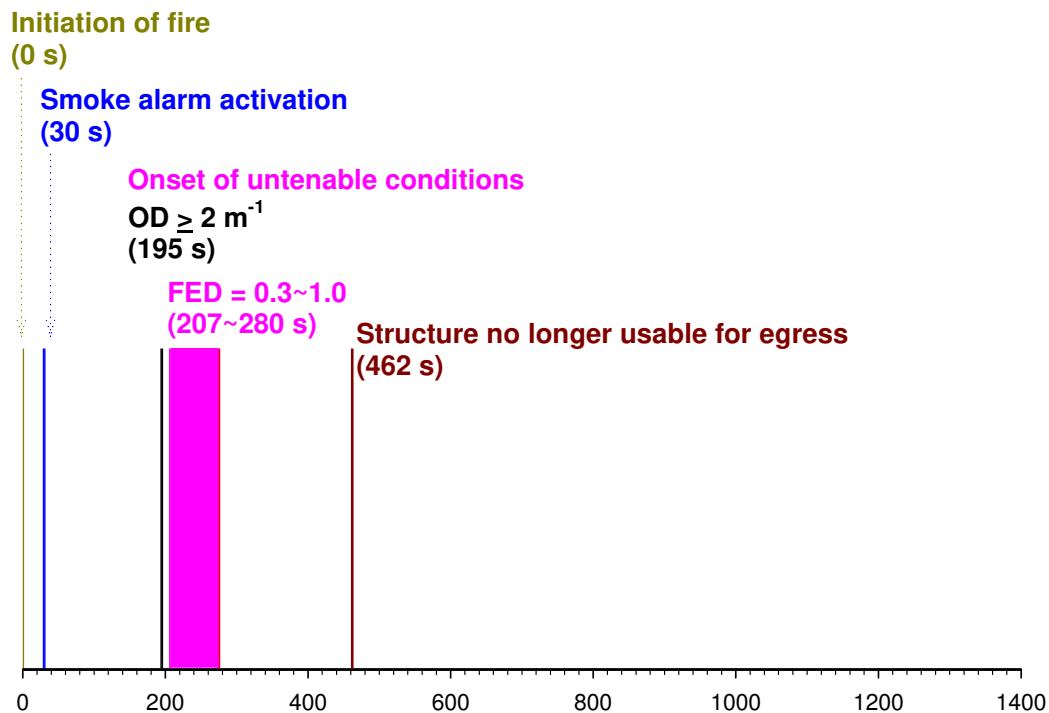**Structure no longer usable for egress (462 s)**

Figure 39. Sequence of fire events in Test UF-04 (s)

4   SUMMARY

This report presents the results and analysis of Test UF-04 as part of the research project on fire performance of houses. The test was conducted in the test facility that simulated a typical two-storey single-family house complying with the minimum code requirements in the NBCC.

A loaded unprotected light-gauge steel C-joist floor (also basement ceilings) was tested using a fire scenario that was characterized in a study documented in reference [6]. A number of measurements were conducted during the tests including temperatures at various locations (in the compartments and on the floor assemblies), fire detection times at various locations, gas measurements, smoke density measurements, flame penetration and deflection measurements for the floor assemblies.

The test was conducted with the open basement doorway (no door in the basement doorway). Under this fire test scenario, structural failure occurred after the onset of untenable conditions (using incapacitation as an end point). The test results must be interpreted within the context of the fire scenario used in the experiment. A relatively severe basement fire scenario was used in the full-scale fire experiment to establish the sequence of the events that would affect the ability of occupants to escape the house in the event of a basement fire.

5   ACKNOWLEDGMENTS

NRC·CNRC

6 REFERENCES

1. Canadian Commission on Building and Fire Codes; National Building Code of Canada; National Research Council of Canada, Ottawa, Canada, 2005.
2. Canadian Commission on Building and Fire Codes, User's Guide – NBC 2005, Application and Intent Statements, National Research Council of Canada, Ottawa, Canada, 2006.
3. Proulx, G., Cavan, N.R., Tonikian, R., Egress Times From Single Family Houses, Research Report 209, Institute for Research in Construction, National Research Council Canada, 2006.
4. Bwalya, A.C., An Extended Survey of Combustible Contents in Canadian Residential Living Rooms, Research Report 176, Institute for Research in Construction, National Research Council Canada, 2004
5. Leroux, P., Kanabus-Kaminska, J.M., Séguin, Y.P., Henrie, J.P., Lougheed, G.D., Bwalya, A.C., Su, J.Z., Bénichou, N., Thomas, J.R. Small-Scale and Intermediate-Scale Fire Tests of Flooring Materials and Floor Assemblies for the Fire Performance of Houses Project, Research Report 211, Institute for Research in Construction, National Research Council Canada, 2007.
6. Taber, B.C., Bwalya, A.C., McCartney, C., Bénichou, N., Bounagui, A., Carpenter, D.W., Crampton, G.P., Kanabus-Kaminska, J.M., Kashef, A., Leroux, P., Lougheed, G.D., Su, J.Z., Thomas, J.R., Fire Scenario Tests in Fire Performance of Houses Test Facility - Data Compilation, Research Report 208, Institute for Research in Construction, National Research Council Canada, 2006.
7. "ASTM E1537-02a: Standard Test Method for Fire Testing of Upholstered Furniture", American Society for Testing and Materials, PA, USA, 2002.
8. Crampton, G.P. The Design and Construction of a Flame Conductivity Device to Measure Flame Penetration through Floor Systems, Research Report 223, Institute for Research in Construction, National Research Council Canada, 2006.
9. Forte, N. and Crampton, P., The Design and Construction of Electronic Deflection Gauges to Measure the Movement of Floor Assemblies in a Fire, Research Report 202, Institute for Research in Construction, National Research Council Canada, 2005.
10. EC1, Eurocode 1, "Basis of design and design actions on structures", Part 2-2: Actions on Structures Exposed to Fire, ENV 1991-2-2, European Committee for Standardization, Brussels, Belgium, 1994.
11. SNZ, "Code of practice for the general structural design and design loadings for buildings", SNZ 4203, Standards New Zealand, Wellington, New Zealand. 1992.
12. AS/NZS, "Structural design actions, Part 0: General principles", AS/NZS 1170.0, Australia/New Zealand Standard, 2002.
13. ASCE 7-98, ASCE Standard, "Minimum design loads for buildings and other structures", American Society of Civil Engineering, Reston, Virginia, 2000.
14. CAN/ULC-S101-04; Standard Methods of Fire Endurance Tests of Building Construction and Materials; Underwriters' Laboratories of Canada, Scarborough, Canada, 2004.
15. ISO Technical Specification 13571, "Life-threatening Components of Fire—Guidelines for the Estimation of Time Available for Escape Using Fire Data," International Organization for Standardization, Geneva, 2002.
16. Purser, D.A., "Toxicity Assessment of Combustion Products," in The SFPE Handbook of Fire Protection Engineering, ed. P.J. DiNenno, D. Drysdale, C.L. Beyler, W.D. Walton, R.L.P. Custer, J.R. Hall, Jr. and J.M. Watts, Jr., 3rd edition,

Society of Fire Protection Engineers /National Fire Protection Association, Quincy, Massachusetts, 2002, Section 2, Chapter 6.

17. Beyler, C., "Toxicity Assessment of Products of Combustion of Flexible Polyurethane Foam," Fire Safety Science -- Proceedings of the Eighth International Symposium, International Association for Fire Safety Science, 2005, pp.1047-1058

18. Laursen, T., "Overview of Toxicity/Effectiveness Issues", Proceedings of Halon Alternatives Technical Working Conference, Albuquerque, NM, 1993, pp. 357-367.

19. Sax, N.I. and Lewis, R.J., "Dangerous Properties of Industrial Materials" (7th ed.), Van Nostrand Reinhold, New York, 1989.

20. Peterson, J.E. and Stewart, R.D., "Predicting the carboxyhemoglobin levels resulting from carbon monoxide exposures," Journal of Applied Physiology, Vol. 39, No. 4, pp. 633-638, 1975

21. Stewart, R.D., Peterson, J.E., Fisher, T.N., Hosko, M.J., Baretta, E.D., Dodd, H.C. and Herrmann, A.A., "Experimental Human Exposure to High Concentrations of Carbon Monoxide," Archives of Environmental Health, Vol. 26, pp. 1-7, 1973

22. Babrauskas, V., "Combustion of Mattresses Exposed to Flaming Ignition Sources, Part I. Full-Scale Tests and Hazard Analysis," NBSIR 77-1290, National Bureau of Standards, Washington, DC, September 1977.

23. Hauck, H. and Neuberger, M., "Carbon monoxide uptake and the resulting carboxyhemoglobin in man," European Journal of Applied Physiology, Vol. 53, pp.186-190, 1984.

24. Gann, R.G., "Estimating Data for Incapacitation of People by Fire Smoke," Fire Technology, Vol. 40, pp.201-207, 2004.

25. Christopher J. Wieczorek and Nicholas A. Dembsey, "Human Variability Correction Factors for Use with Simplified Engineering Tools for Predicting Pain and Second Degree Skin Burns", Journal of Fire Protection Engineering, Vol. 11, No. 2, 88-111, 2001

26. Jin, T., "Visibility and Human Behavior in Fire Smoke," in The SFPE Handbook of Fire Protection Engineering, ed. P.J. DiNenno, D. Drysdale, C.L. Beyler, W.D. Walton, R.L.P. Custer, J.R. Hall, Jr. and J.M. Watts, Jr., 3rd edition, Society of Fire Protection Engineers /National Fire Protection Association, Quincy, Massachusetts, 2002, Section 2, Chapter 4.

27. Babrauskas, V., "Full-Scale Burning Behavior of Upholstered Chairs," NBS Technical Note 1103, National Bureau of Standards, Washington, DC, August 1979.

28. Bukowski, R.W., Peacock, R.D., Averill, J.D., Cleary, T.G., Bryner, N.P., Walton, W.D., Reneke, P.A., Kuligowski, E.D., "Performance of Home Smoke Alarms - Analysis of the Response of Several Available Technologies in Residential Fire Settings," NIST Technical Note 1455, National Institute of Standards and Technology, December 2003.

29. Su, J., Bwalya, A., Lougheed, G., Bénichou, N., Taber, B., Kashef, A., Leroux, P. and Thomas, R., Fire Scenario Tests In Fire Performance Of Houses Test Facility – Data Analysis, Research Report 210, Institute for Research in Construction, National Research Council Canada, 2007.

Table A 1. Test Summary for Test UF-04

- Test ID: UF-04
- Test Date: March 23, 2006
- Atmospheric Conditions: Temp: 2^{O}C   RH: 80%   Pres: 102.1 kPa↑
- Structure Tested:
  Steel C-joist, 203 x 32 x 1.438
  15.1 mm (5/8") OSB floor
  0.95 kPa load (144 concrete blocks, 2490 kg, 61 m pipe, 143 kg)

- Fire Load:
  Mock-up sofa at centre of basement (9.10 kg foam)
  Wood crib located 200 mm behind mock-up sofa (57.8 kg, ≤6% MC)
  Wood crib located 200 mm from west side of mock-up sofa (60.2 kg, ≤6% MC)
  Two wood cribs located under the mock-up sofa (30.4 kg, 28.7 kg, ≤6% MC)
  80 s ignition with 19 kW burner (13 l/min)

- Ignition time after start of data: <u>1:00</u>

- Doors: SE bedroom door closed / SW bedroom door open
    Door at top of basement stairs open
    first floor exterior door opened at 3:00 after ignition

- Window: Window opened at <u>2:00</u> after ignition (300 ^{O}C)

- Floor collapse: <u>7:42</u> (462 s) after ignition

- Smoke Detector Activation Times:

	Activation *(time from ignition)*
Smoke Detector #2, Photoelectric, Basement, bottom of stairs	30 s
Smoke Detector #3, Ionization, 1st Floor, top of stairs	65 s
Smoke Detector #4, Photoelectric, 1st Floor, top of stairs	85 s
Smoke Detector #5, Ionization, 2nd Floor, top of stairs	115 s
Smoke Detector #6, Photoelectric, 2nd Floor, top of stairs	130 s
Smoke Detector #7, Ionization, SE bedroom, closed	230 s
Smoke Detector #8, Photoelectric, SE bedroom, closed	250 s
Smoke Detector #9, Ionization, SW bedroom, open	160 s
Smoke Detector #10, Photoelectric, SW bedroom, open	225 s

NRC·CNRC